C.P. No. 1019

C.P. No. 1019

MINISTRY OF TECHNOLOGY

AERONAUTICAL RESEARCH COUNCIL

CURRENT PAPERS

On the Driver-Reservoir Technique

Part 1 Application to Shock and Gun Tunnels

By

L. Davies and K. Dolman

Part 2 Determination of Optimum Reservoir Size

By

L. Davies, D. R. Brown and G. Hooper

LONDON: HER MAJESTY'S STATIONERY OFFICE

1968

TEN SHILLINGS NET

C.P. No. 1019*

January 1968

On the Driver-Reservoir Technique

Part 1 - Application to Shock and Gun Tunnels

By L. Davies and K. Dolman

SUMMARY

The driver-reservoir technique, first proposed by Henshall et al, is of interest to shock tunnel users because of its promise of an increase in running time. The most usual form of termination of running time in the shock tunnel is by the arrival, at the end plate, of the head of the rarefaction wave which results from the rupture of the main diaphragm. In the driver-reservoir technique, the head of the rarefaction wave interacts with a perforated plate, at the end of the high pressure chamber, which separates this chamber from a larger diameter vessel called the reservoir. Under certain conditions this results in no waves propagating downstream except Mach waves. The head of the expansion wave has therefore been effectively eliminated and this will result in an increasein running time.

In this paper an account of the driver-reservoir technique is given, together with various theoretical analyses. A simple model is proposed which describes the wave processes within the reservoir, and the increase in running time to be expected from various sizes of reservoir. From this model it is shown that the most important reservoir dimension is the diameter. Experiments from the NPL 2 in. shock tunnel are presented, and the application of the technique to gun tunnels is discussed.

List of Contents

* Replaces NPL Aero Reports 1226, 1255 (A.R.C.28 957, 29 857)

Nomenclature

A	cross-sectional area of reservoir
A_c	cross-sectional area of channel of shock tunnel
A_n	shock-tunnel nozzle throat area
A_t	area of hole(s) in perforated plate
a	speed of sound
a_{ij}	a_i/a_j
d	diameter of driver and channel of shock tunnel
d^*	diameter of gun-tunnel nozzle throat
L	length of driver section of shock tunnel
L'	length of driven section of shock tunnel
M	u/a, Mach number
M_1	Mach number of flow in reservoir, see Fig. 6
M_c	Mach number of primary shock which produces 'crossover' conditions, see Fig. 4
M_s	primary shock Mach number
M_T	primary shock Mach number for tailored operation
m	molecular weight
p	pressure
p_{ij}	p_i/p_j
p'_{3u}/p_4	pressure ratio across an unsteady expansion
p_{3s}/p_4	pressure ratio across a steady expansion
p_e	equilibrium pressure in reservoir of gun tunnel
T	temperature
T_e	equilibrium temperature in reservoir of gun tunnel

t/

t	time
U_{ij}	u_i/a_j
u	flow velocity
V	volume of driver reservoir
α	$(\gamma + 1)/(\gamma - 1)$
γ	c_p/c_v, specific heat ratio
δ	ratio of A_t/A_c
δ_x	area ratio for 'crossover' conditions shown in Fig. 4
δ^*	area ratio defined by equation 11
δ_{IDEAL}	area ratio which produces no downstream running waves except Mach waves

Subscripts

1,2,3,4	refer to regions shown in Fig. 1
3s	conditions produced across a steady expansion
3u	conditions produced across an unsteady expansion

---

1. Introduction

The extreme brevity of the available testing time in shock tunnels makes the task of taking measurements of the flow very difficult. Transducers have to be capable of sub-millisecond response and yet be sensitive enough to make measurements, for example, of pressures in the millimeter Hg range. Any technique which will increase the duration of testing time whilst maintaining the integrity of the working-section flow is therefore of great importance.

One such technique has been proposed by Henshall et al[1]. The basis of this method is that a vessel of larger diameter than the driver section is connected to the end of the driver and separated from it internally by a perforated plate (see Figs. 1 and 2). The head of the expansion wave, produced when the main diaphragm bursts, interacts with this perforated plate. A complex flow situation results, leading to no waves propagating downstream, except Mach waves, when certain conditions are fulfilled. Since it is the arrival of the reflected head of the expansion wave at the end of the shock tube which normally terminates the flow in the reflected shock tunnel, effective elimination of this wave should result in an increase in running time.

In/

In this paper an account is given of the analysis of the driver-reservoir technique as proposed by Flagg[2], and this is compared with experiments in the NPL 2 in. shock tunnel, using helium and nitrogen as driver gases and nitrogen as test gas. The driver pressure ranged from 1000 to 10 000 psi at room temperature. An extension of this technique to gun-tunnel use is also discussed.

2. Theory

2.1 Analysis of driver reservoir technique

In simple shock-tunnel flow (shown in Fig. 1) the testing time is usually terminated by the arrival of the head (or tail) of the expansion wave from the high pressure end of the tube. Techniques for increasing the running time might, as a start, aim at delaying the arrival of these waves at the nozzle entrance. One possibility is to lengthen the driver section, thus increasing the time spent by the expansion wave in travelling through this section. For an appreciable increase in testing time however this becomes impracticable. An alternative technique has been developed by Henshall et al[1]. In this method a reservoir of larger diameter than the driver is connected to the end of the driver section and separated from it internally by means of a perforated plate. The head of the expansion wave interacts with this plate and from the complex flow which develops no downstream propagating waves, except Mach waves, will result when certain conditions are fulfilled. These conditions are derived by Flagg[2] in his analysis of the driver-reservoir technique, and a brief description of this analysis will now be given.

In his analysis Flagg has elected to use the (p,u) plane method rather than the more laborious method of characteristics, and explains that this former method will give all the required information about the resulting quasi-steady states. He points out however that for a detailed study of the wave processes, which would be desirable in order to establish how the final wave systems are formed, it is of course necessary to use the method of characteristics. Although the (p,u) plane method takes no account of the secondary interaction of characteristics, Flagg notes that the method is valid as long as the strengths of the waves involved are not extreme, and mentions that subsequent experimental data gave good agreement with this simple theoretical approach.

The driver-reservoir system when set up in the laboratory is shown schematically in Fig. 2. When the main diaphragm ruptures, the gas initially at rest between the main diaphragm and the perforated plate undergoes an unsteady expansion to a new state determined by the initial conditions. The gas initially at rest in the reservoir undergoes a steady expansion to a condition determined by the area ratio of the perforated plate. Flagg describes the pressure ratio across an unsteady expansion when the gas is initially at rest by the expression:

$$\frac{p'_{3u}}{p_4} = \left[1 - \frac{(\gamma_4 - 1)U'_{3u}}{2a_4}\right]^{\frac{2\gamma_4}{\gamma_4 - 1}} \quad ...(1)$$

and/

and the pressure ratio across a steady expansion when the gas is initially at rest by:

$$\frac{p_{3s}}{p_4} = \left[1 - \frac{(\gamma_4 - 1)}{2}\left(\frac{U_{3s}}{a_4}\right)^2\right]^{\frac{\gamma_4}{\gamma_4 - 1}} . \qquad \ldots(2)$$

From Fig. 4, which is reproduced from Flagg's paper, it is shown that the two expansions produce the same end point in the (p,u) plane at only one point other than the initial one. This point is found by equating (1) and (2) above, which gives:

$$\left[1 - \frac{(\gamma_4 - 1)U_{3u}}{2a_4}\right]^2 = 1 - \frac{\gamma_4 - 1}{2}\left(\frac{U_{3s}}{a_4}\right)^2 \qquad \ldots(3)$$

where $U_{3u} = U_{3s} = U_s$.

Solving for u where

$$\frac{U_s}{a_4} = \frac{4}{\gamma_4 + 1}, \; M_s = \frac{4}{3 - \gamma_4} .$$

This analysis, Flagg notes, shows that very rigid restrictions are set on the initial conditions if both the tailoring and crossover requirements are to be met. The term "crossover point" is applied to the point shown in Fig. 4 where the steady and unsteady expansions produce the same end point. Flagg only considers the tailored mode of operation.

In order to compute the necessary conditions for eliminating the reflected head of the expansion wave, it is first required that the ratio M_T/M_C be determined, where M_T and M_C are the tailored Mach number and the crossover condition Mach number respectively (see Fig. 4). The crossover Mach number is that which is obtained under the conditions described for the crossover point in Fig. 4.

The condition which has to be satisfied for tailored interface operation is:

$$\frac{m_3}{m_2}\frac{(\gamma_3 - 1)}{(\gamma_2 - 1)} \cdot \frac{T_2}{T_3} = \left(\frac{\alpha_2 + P_{25}}{\alpha_3 + P_{25}}\right) \qquad \ldots(4)$$

where $\alpha = \dfrac{\gamma + 1}{\gamma - 1}$ and m = molecular weight.

The so-called crossover Mach number is given by the expression:

$$M_C = \frac{\gamma_1 + 1}{\gamma_4 + 1} \cdot a_{41} + \left[\left(\frac{\gamma_1 + 1}{\gamma_4 + 1}\right)^2 a_{41} + 1\right]^{\frac{1}{2}} . \qquad \ldots(5)$$

It/

It is then only necessary, by inspection, to determine whether the ratio M_T/M_C is greater than, equal to or less than unity. For most practical cases, e.g., with helium, hydrogen or combustion gases as driver gases and air or nitrogen as driven gas, the ratio is less than unity. Flagg notes that the cases $M_T/M_C = 1$ and $\frac{M_T}{M_C} > 1$ are not realistic and only $\frac{M_T}{M_C} < 1$ applies in practice. For this case the ratio of the hole area to the cross-sectional area of the driver which is required to eliminate the reflected head of the expansion wave is given by:

$$\delta = \left(\frac{\gamma_4 + 1}{2}\right)^{\frac{\gamma_4 + 1}{2(\gamma_4 - 1)}} \frac{U_{3s}}{a_4}\left[1 - \frac{\gamma_4 + 1}{2}\left(\frac{U_{3s}}{a_4}\right)^2\right]^{\frac{1}{\gamma_4 - 1}} \qquad \text{...(6)}$$

and this is solved by using the relationships:

$$\frac{U_{3u}}{a_4} = \frac{2}{a_{41}(\gamma_1 + 1)}\left(M_T - \frac{1}{M_T}\right) \qquad \text{...(7)}$$

$$\frac{p_{3u}}{p_4} = \left(1 - \frac{\gamma_4 - 1}{2}\frac{U_{3u}}{a_4}\right)^{\frac{2\gamma_4}{\gamma_4 - 1}} \qquad \text{...(8)}$$

$$\frac{U_{3s} - U_{3u}}{a_4}\left(\frac{a_4}{a_3}\right) = \left[\frac{2}{\gamma_4(\gamma_4 - 1)}\right]^{\frac{1}{2}} \frac{\frac{p_{3u}p_4}{p_4 p_{3s}} - 1}{\left[1 + \frac{\gamma_4 + 1}{\gamma_4 - 1}\cdot\frac{p_{3u}}{p_4}\cdot\frac{p_4}{p_{3s}}\right]^{\frac{1}{2}}} \qquad \text{...(9)}$$

and

$$\frac{a_3}{a_4} = \left[1 - \frac{\gamma_4 - 1}{2}\left(\frac{U_{3s}}{a_4}\right)^2\right]^{\frac{1}{2}} \qquad \text{...(10)}$$

together with equation (2).

Some curves of δ_{IDEAL} versus driven gas specific heat ratio, for given driver gas specific heat ratio, are reproduced from Flagg's report and shown in Fig. 5. From a comparison of experiment and theory it is found that Flagg's analysis provides a useful rule of thumb for estimating roughly the area ratio δ required. It is then necessary to carry out a series of tests to determine the exact value. In this respect a semi-empirical equation obtained by the present authors, using momentum conservation principles, would appear to provide an equally useful rule of thumb value for determining the required area ratio. This formula is:

δ*/

$$\delta^* = \left(\frac{P_{21}}{P_{41}}\right)^{\frac{1}{\gamma_4}} \cdot \left(\frac{U_{21}}{A_{41}}\right) \cdot \left(\frac{2}{\gamma_4 + 1}\right)^{-\left(\frac{\gamma_4 + 1}{2(\gamma_4 - 1)}\right)} \qquad \ldots(11)$$

and is readily used in connection with tables of P_{41}, P_{21}, U_{21}, A_{41} as produced by Bernstein[5] for example. A comparison of the predicted values of δ obtained from equations (6) and (11) and with experiment is given in Table 1.

Table 1

Driver Gas / Driven Gas	M_s	(FLAGG) δ_x	(FLAGG) δ_{IDEAL}	DAVIES & DOLMAN δ^*	EXP δ_{EXP}
H_2/N_2	6•02	0•379	0•382	0•337	0•333 (Ref. 1)
H_e/N_2	3•4	0•333	0•351	0•435	0•380 (N.P.L.)
N_2/N_2	2•0	0•379	Not Applicable	0•439	0•39 (N.P.L.)

Taking the values from the above table, the percentage deviation of the various theoretical predictions from the experimental values can be estimated from the ratios presented below.

	$\frac{(\delta_x)_{FLAGG}}{\delta_{EXP}}$	$\frac{(\delta_{IDEAL})_{FLAGG}}{\delta_{EXP}}$	$\frac{(\delta^*)_{DAVIES\ DOLMAN}}{\delta_{EXP}}$
H_2/N_2	1•137	1•146	1•011
H_e/N_2	0•876	0•9236	1•14
N_2/N_2	0•97	Not Applicable	1•125

For the NPL 2 in. Gun Tunnel with N_2 as driver and test gas, the predicted value of δ, using equation (11) is 0•4466, whereas the experimental value was found to be 0•4306.

2.2/

2.2 The increase in running time obtained using the driver reservoir

Although various features of the flow which result from the interaction of the head of the expansion wave with the perforated plate have been described, no solution to the flow within the reservoir, and hence a prediction of the expected running time, has been given. A semi-empirical approach has been adopted by Henshall et al, but Flagg has not treated this part of the problem.

In their paper Henshall et al postulate that the ratio of the gain in test time $\Delta\tau$, due to the use of the driver reservoir, to the test time in the conventional tunnel (τ) is given by the following relationship:

$$\frac{\Delta\tau}{\tau} = f\left(\frac{L'}{L}, M_s, \frac{A_o}{A_n}, \frac{V}{L'd^2}\right). \qquad \ldots(12)$$

Henshall's experiments showed that the tail of the expansion wave did not affect the running time, and the head of the expansion wave had been effectively eliminated. Therefore the running time was dependent only on the arrival of the contact surface at the working section nozzle throat. Henshall et al suggest that the effectiveness of the reservoir is terminated by the breakdown of the constant mass flow through the plate. The simple approach adopted in this paper is to assume that the flow in the reservoir is initiated by the passage of the expansion head into the reservoir and that thereafter there are no other external influences. The flow situation is shown in Fig. 6. The first possible interruption to constant conditions at the plate will then be due to the arrival of the expansion head reflected from the end of the reservoir. The time taken for the expansion to arrive back at the plate (t) has been calculated by Cable and Cox[3], and this is given by the relationship:

$$\frac{t}{t_o} = \frac{2}{(1 + M_1)}\left\{1 + \frac{\gamma - 1}{2} M_1\right\}^{(\gamma + 1)/\{2(\gamma - 1)\}} \qquad \ldots(13)$$

where t_o is the time taken for a disturbance travelling at the speed of sound in the reservoir to travel the length of the reservoir assuming the gas to be at rest. M_1 is given by the equation

$$\frac{A}{A_t} = \frac{1}{M_1}\left\{\frac{1 + \frac{\gamma - 1}{2} M_1^2}{\frac{\gamma + 1}{2}}\right\}^{(\gamma + 1)/\{2(\gamma - 1)\}} \qquad \ldots(14)$$

where A is the reservoir cross-sectional area, and A_t is the area of the hole in the perforated plate. A curve of t/t_o for various M_1 and A/A_t, and for $\gamma = 1{\cdot}4$, is reproduced from the paper by Cable and Cox in Fig. 7. From this curve it can be seen that the time the expansion takes to reach the

plate,/

plate, after starting the flow is nearly twice the time taken to reach the end of the reservoir. In the NPL 2 in. Shock Tunnel when using nitrogen as test gas, this time is about 5 ms, and in the experiments of Henshall et al is approximately 400 μs. Both these times are far shorter than the experimentally observed increase in running time. It is found however that the pressure drop across this first expansion is very small, and would not cause a breakdown in the flow through the nozzle*, although a weak expansion may be propagated downstream.

The fall in pressure in the reservoir due to successive reflections of the expansion wave has also been calculated by Cable and Cox, and their expression for the pressure after the n^{th} reflection, as a ratio of the initial pressure in the reservoir, is given as:

$$\frac{p_n}{p_4} = \left\{\frac{1 - \frac{\gamma - 1}{2} M_1}{1 + \frac{\gamma - 1}{2} M_1}\right\}^{\frac{2\gamma(n-1)}{\gamma - 1}} \frac{1}{\left\{1 + \frac{\gamma - 1}{2} M_1\right\}^{2\gamma/(\gamma - 1)}} \quad \ldots (15)$$

Table 2 shows the results, for the NPL 2 in. Shock Tunnel reservoir, of successive reflections of the expansion wave and the pressures associated with these reflections. From this table it is seen that the pressure drop across the first few reflections is very small.

Table 2

Reflection	p_n/p_4
2nd	0·914
3rd	0·894
4th	0·8747
5th	0·79
6th	0·73
7th	0·66
8th	0·6

From equation (15), it is clear that for decreasing values of M_1 the pressure drop across successive reflections also decreases. The value of M_1 is determined by the area ratio A/A_t. In the experiments carried out by

Henshall et al,/

*Flow breakdown is defined as termination of constant conditions at the perforated plate when the pressure in the reservoir falls below the critical value.

Henshall et al, this ratio is very large, or in terms of Fig. 7 the reciprocal is very small and so M_1 will be small. This will result in very weak expansion waves for the first few reflections and perhaps explains why the pressure records obtained by Henshall et al remain so steady over the testing time. Evidence of expansion waves being propagated downstream before the breakdown of flow at the perforated plate is more evident on the records obtained in the NPL 2 in. Shock Tunnel where A_t/A, and therefore M_1, are larger, resulting in larger pressure drops across the expansion waves (see equation (15)).

From this rather simple approach certain predictions can be made. Extending the length of the reservoir will delay the arrival of the first reflection from the end of the reservoir, but this is a return to the situation which existed before the use of the driver reservoir. The best use of the driver reservoir will be made where space is at a premium in the laboratory, and then when the cross-sectional area of the reservoir is very much greater than the area of the perforation in the dividing plate between the reservoir and the driver, in fact the situation originally devised by Henshall et al. The reservoir in use in the NPL 2 in. Shock Tunnel is not as satisfactory because the ratio A_t/A is not small enough. Finally, from Table 2 it may be inferred that flow breakdown will not occur for a time less than four or five times t/t_0. When the ratio A_t/A is much smaller than the NPL 2 in. Shock Tunnel value, this time will be correspondingly longer.

2.3 Application of the driver-reservoir technique to gun-tunnel operation

In gun-tunnel operation, as in shock-tunnel operation, the head or tail of the expansion wave is often a deciding factor in determining the running time. In order to make full use of the available running time, determined by the time taken for all the gas between the piston and the end plate to flow through the nozzle into the working section, the expansion head (or tail) should not arrive before a time τ_g given by the formula:

$$\tau_g = \frac{L}{P_{41} P_{e4} a_1} \cdot \left(\frac{T_e}{T_1}\right)^{\frac{1}{2}} \cdot \left(\frac{d}{d^*}\right)^2 \cdot \left(\frac{2}{\gamma + 1}\right)^{-\frac{\alpha}{2}} . \qquad \ldots(16)$$

One means of ensuring this is to use the driver-reservoir technique. Since in simple gun-tunnel flow theory the piston is assumed to accelerate quickly to the contact-surface velocity and certain features of the flow are calculated using this analogy, the value of δ required for driver-reservoir operation is computed as for the equivalent shock tunnel, using equation (6) or (11).

This has been done for the NPL 2 in. Gun Tunnel and the results are described below.

A disturbing feature of the use of gun tunnels at very high pressures is the high peak pressure caused by the reflection of the shock produced as the piston slows to rest.[6] As the piston slows down a shock wave is produced (see Fig. 8) which travels back to the driver section, reflects and on reaching

the/

the piston produces a high pressure peak in the gas between the piston and the end face. These pressure peaks can be so high at the highest operating pressures as to be prohibitive. However when a driver reservoir is being used, this shock, on reaching the end of the driver section, encounters and interacts with the perforated plate. The result is that the shock is much weakened and reductions in shock strength of up to about 80% have been achieved (see Fig. 9). In these records the top trace is pitot pressure taken in the working section, and the bottom trace is the reservoir pressure. The shock, produced by piston deceleration, which is reduced occurs near the end of the trace, as indicated (A), and the extent of the reduction is clearly seen in the lower record. It may be concluded that not only does the driver reservoir offer the possibility of making full use of the available running time in gun tunnels, especially where there is not enough space for a long driver section, but may also be said to be an essential feature of high-pressure operation.

3. Experimental Work

3.1 Shock-tunnel details

The NPL 2 in. Shock Tunnel has a 12 ft long low-pressure channel and originally had a 10 ft driver chamber made up of a 7 ft length and a 3 ft length. In order to examine the driver-reservoir technique the last 3 ft of the chamber furthest away from the main diaphragm were replaced by a 4 in. internal diameter, 3 ft long reservoir (see Fig. 3). Inside the tube the original chamber section is divided from the reservoir by means of a 0·1 in. thick steel plate with a central hole. The end of the reservoir rests against a hydraulic ram which closes the tunnel with a force of 30 tons. The retractor springs are clearly seen around the tube and two smaller ones either side of the reservoir. Fuller details of the tunnel may be obtained from Ref. 4.

3.2 Shock-tunnel tests with helium as driver and nitrogen as test gas

The results of the matching of the open to total area of the perforated plate were judged from an examination of the reflected shock pressure records, as was done by Henshall et al[1]. If the hole is too small, then an expansion wave is propagated down the tube (Fig. 10a). If the hole is too large then the right running wave is a compression wave (Fig. 10b). Ideally the correct hole size should produce no right running wave, except a Mach wave. This was not obtained in practice, however, and the best match was judged to be that shown in Fig. 10c, where it can be seen that a small compression wave occurs. In all the records no absolutely level section is obtained after the first disturbance from the perforated plate, even at the 'matched' condition. This tends to support the simple analysis proposed in Section 2.2, where it was suggested that even when the correct value of δ was used, weak expansion waves would be propagated downstream as a result of reflections of the head of the expansion wave within the reservoir. In Fig. 10c there are clear signs of this occurring. In order to minimise this effect, it would be necessary to increase the diameter of the reservoir. This would then reduce the ratio A_t/A, leading to an associated reduction in M_1, and consequently a reduction in the pressure drops across the reflected expansions which occur in the reservoir. When the driver pressure was raised from 1000 to 10 000 psi, the perforated plate still performed its task of eliminating the reflected head of the expansion, and appeared not to be influenced by bulk compressibility effects (see Fig. 10d). An effective increase of about 2 ms in running time was achieved and a comparison of pressure records before and after using the technique is shown in Fig. 10g.

3.3/

3.3 Shock-tunnel tests with nitrogen as driver and test gas

The tests were repeated with nitrogen as both driver and test gas and again the correct value of δ, as judged from the pressure records (Fig. 10f), did not produce a perfectly level trace. Here again the diameter of the reservoir should be increased.

In both the helium and nitrogen tests the working-section flow was examined, and a flat plate heat transfer trace is shown in Fig. 10e for $H_e : N_2$ operation. From this trace it seems that the running time has been effectively increased, and with the above suggested modification to reservoir geometry the flow should be useful for extended duration testing. In fact the flow is perhaps good enough for this purpose already, and should improve with increase in reservoir diameter.

4. Conclusions

(a) The flow which develops as a consequence of the interaction of the head of the expansion wave with the perforated plate, in driver-reservoir operation, is sufficiently known to enable a reasonably close prediction of the size of the hole(s) in the perforated plate to be calculated, for special predetermined operating conditions.

(b) At the matched conditions no right running waves except Mach waves result from the interaction of the expansion wave head with the perforated plate. The reflected expansion wave head is therefore effectively eliminated.

(c) The extra running time obtained will depend on the geometry of the reservoir. The expansion wave which passes into the reservoir will reflect from the end of the reservoir and from the perforated plate, alternately, causing a reduction in the pressure in the reservoir. Several reflections are required to reduce the reservoir pressure to the critical pressure at the perforated plate, and so terminate the effectiveness of the reservoir. At each reflection at the plate, weak expansion waves pass through the plate holes and propagate downstream. The strength of these waves depends on the ratio of the area of the hole(s) in the perforated plate to the cross-sectional area of the reservoir. For most effective operation this ratio should be made as small as possible.

(d) The driver reservoir technique can also be used effectively in gun-tunnel operation. In fact it is suggested that for very high pressure gun-tunnel operation, the driver-reservoir technique, or a similar arrangement, may be essential in order to reduce the strength of the reflection, at the plate, of the shock produced as the piston slows to rest.

(e) As a result of this investigation it is considered that an experimental investigation into the effect of different diameter reservoirs on the flow should prove most instructive.

Acknowledgements

This project was initially suggested by Dr. L. Pennelegion. The detailed design of the driver reservoir was by Mr. J. Godwin in the Design Office, and the construction and assembly in the division workshops was the responsibility of Mr. J. Darcy.

References/

References

No.	Author(s)	Title, etc.
1	B. D. Henshall, R. N. Teng and A. D. Wood	Development of very high shock tunnels with extended steady-state test times. AVCO Tech. Rep. RAD-TR-62-16. (1962).
2	R. F. Flagg	A theoretical analysis of the driver-reservoir method of driving hypersonic shock tunnels. UTIAS Tech. Note No.93. April, 1965.
3	A. J. Cable and R. N. Cox	The Ludwieg pressure-tube supersonic wind tunnel. Aeronaut. Q., Vol.XIV, 1963, pp.143-157.
4	L. Davies, L. Pennelegion, P. Gough and K. Dolman	The effects of high pressure on the flow in the reflected shock tunnel. A.R.C. C.P. 730, September, 1963.
5	L. Bernstein	Tabulated solutions of the equilibrium gas properties behind the incident and reflected normal shock wave in a shock tube. I - Nitrogen. II - Oxygen. A.R.C. C.P. 626, April, 1961.
6	East, R. A. and Perry, J. H.	A study of the characteristics of gun tunnel operation at 10 000 lb/in.^{2} AASU Report No. 268. April, 1967.

HD

FIG. I

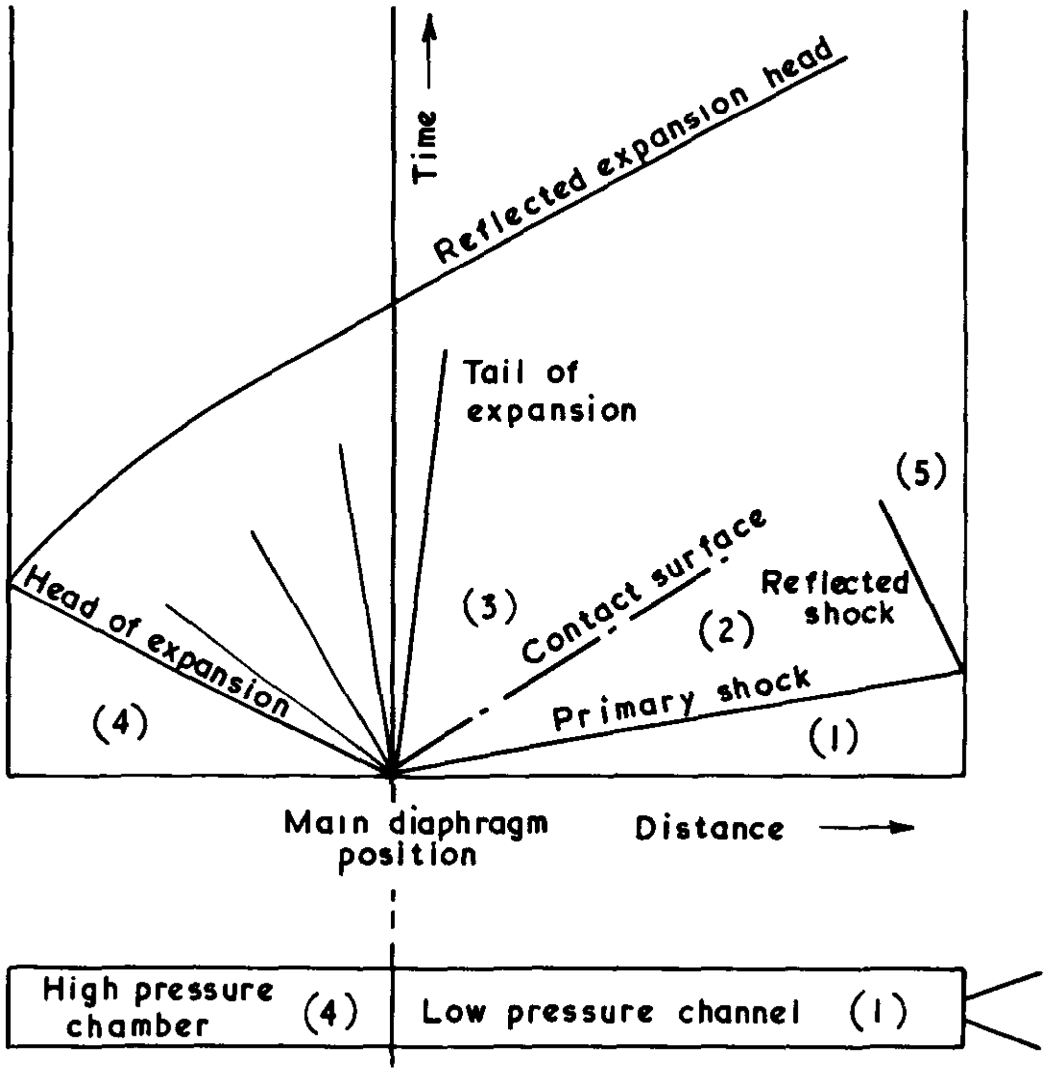

Simple shock tunnel flow diagram

FIG. 2

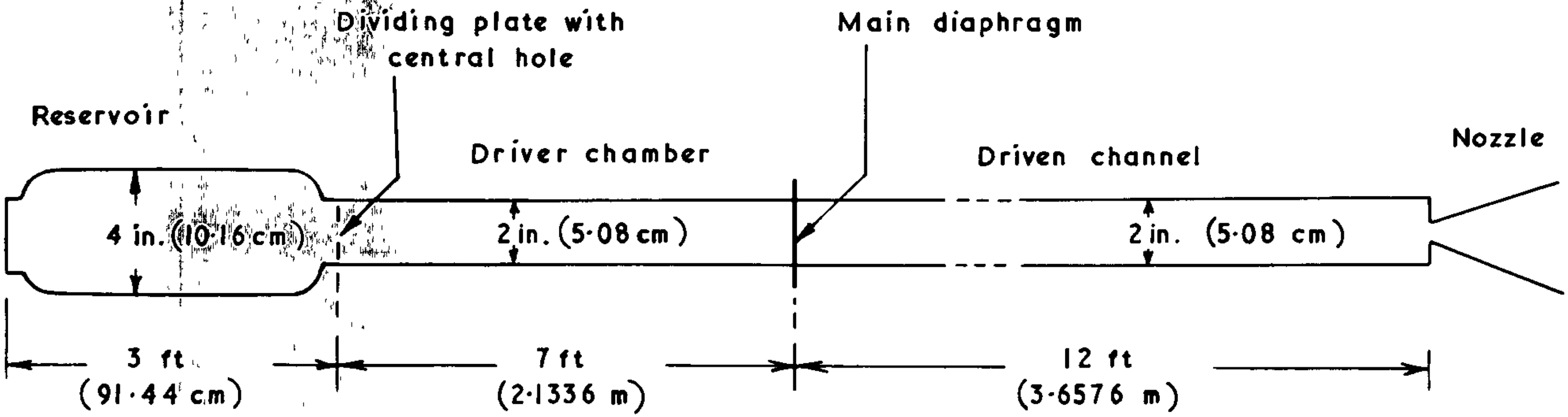

Schematic diagram of 2 in. (5·08 cm) shock tunnel with reservoir attachment

FIG. 3

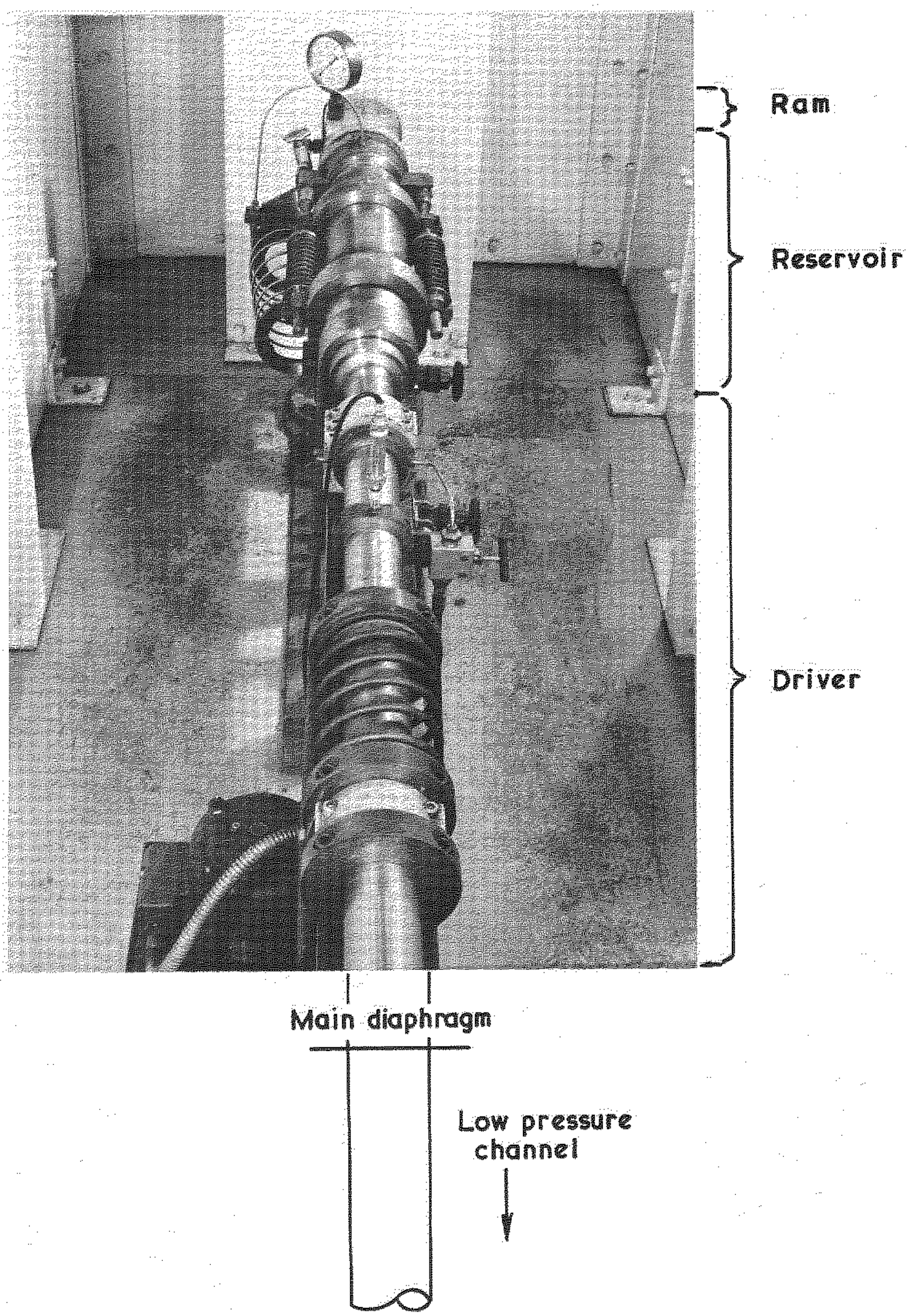

Photograph of high pressure section NPL 2 in. shock tunnel with reservoir attachment.

FIG. 4

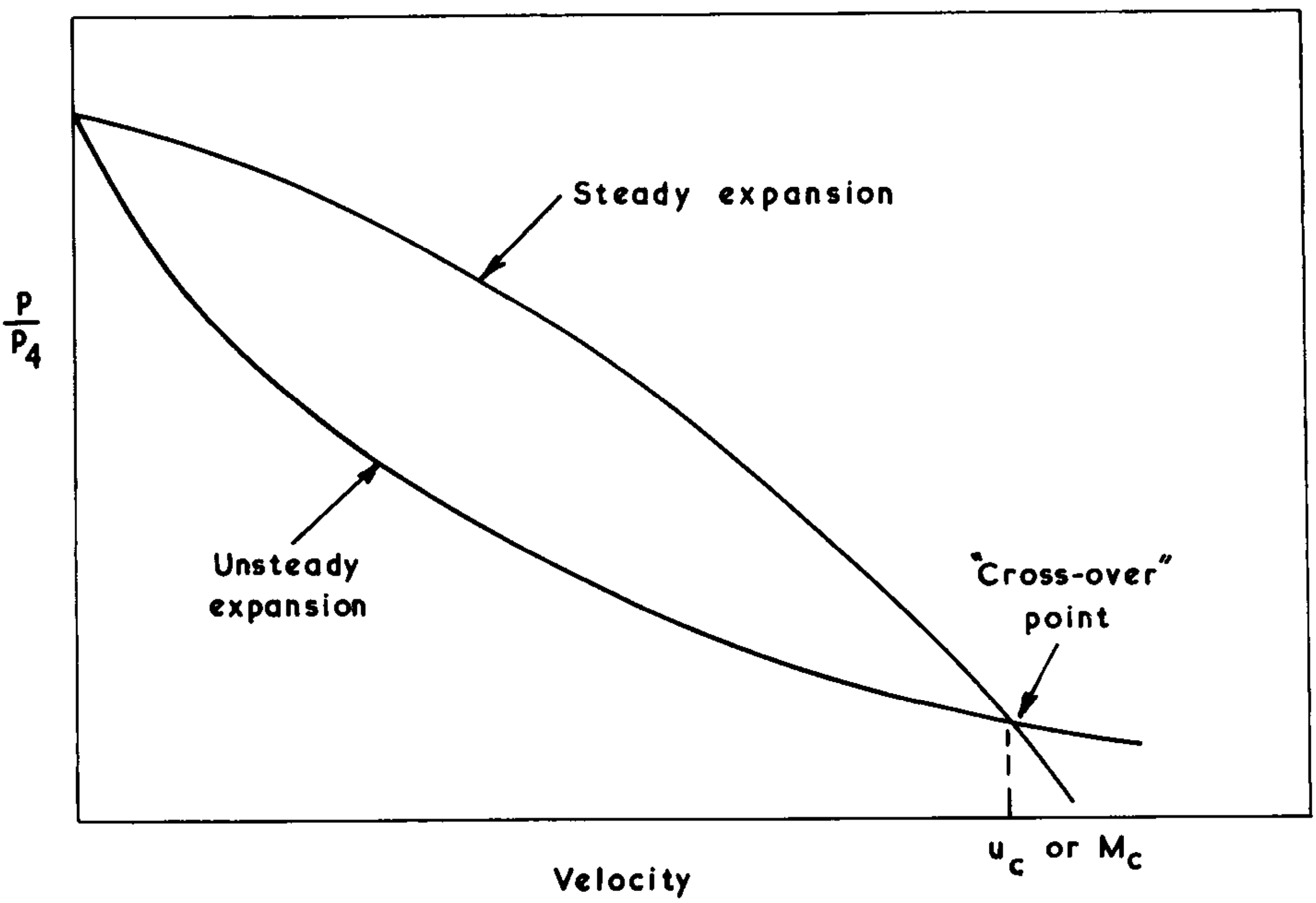

Diagrammatic representation of characteristics of steady and unsteady expansions on the (p, u)-plane.

(After Flagg: see Ref. 2)

FIG. 5

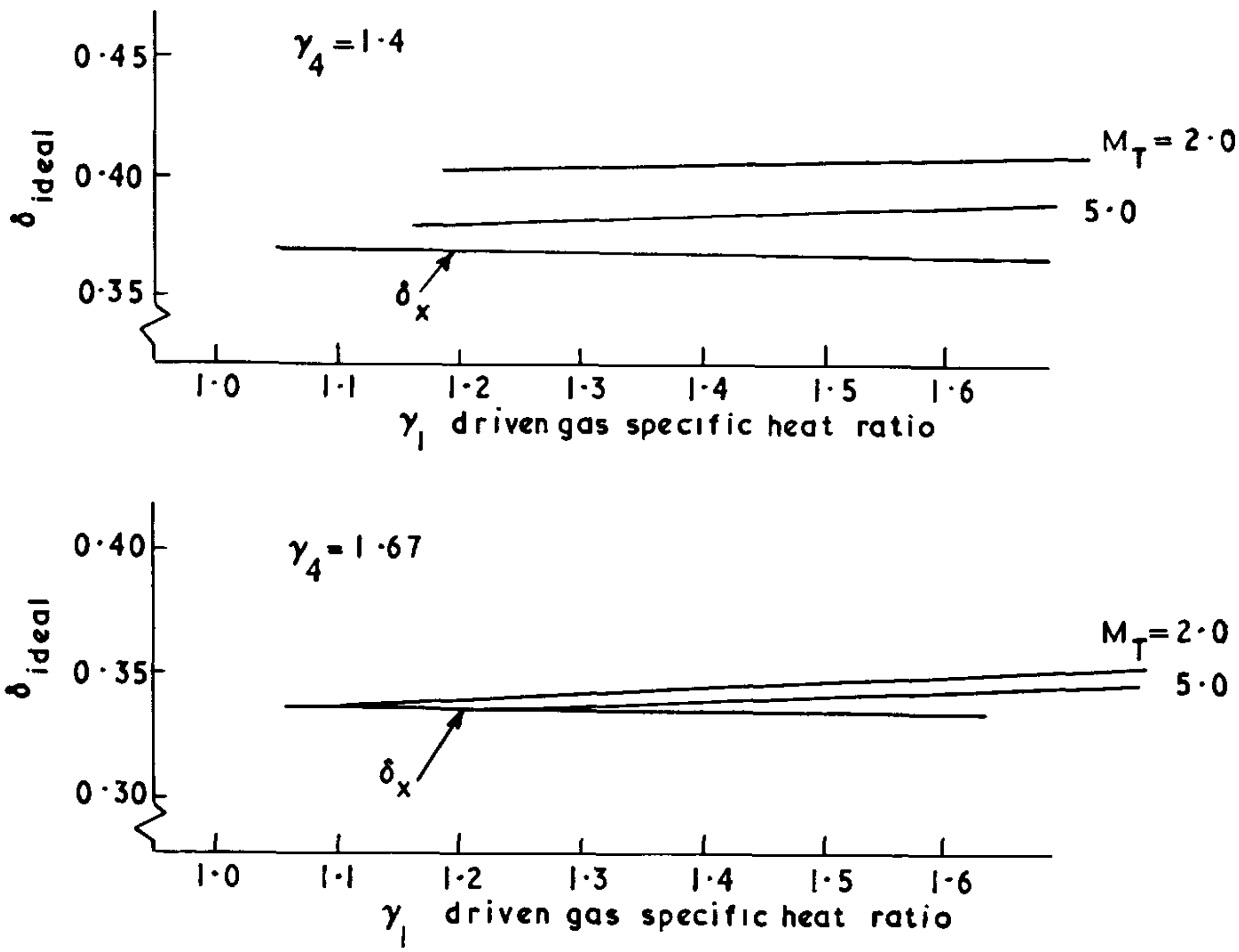

Ideal perforated plate hole area ratio vs. driven gas specific heat ratio.

(After Flagg: Ref 2)

FIG. 6

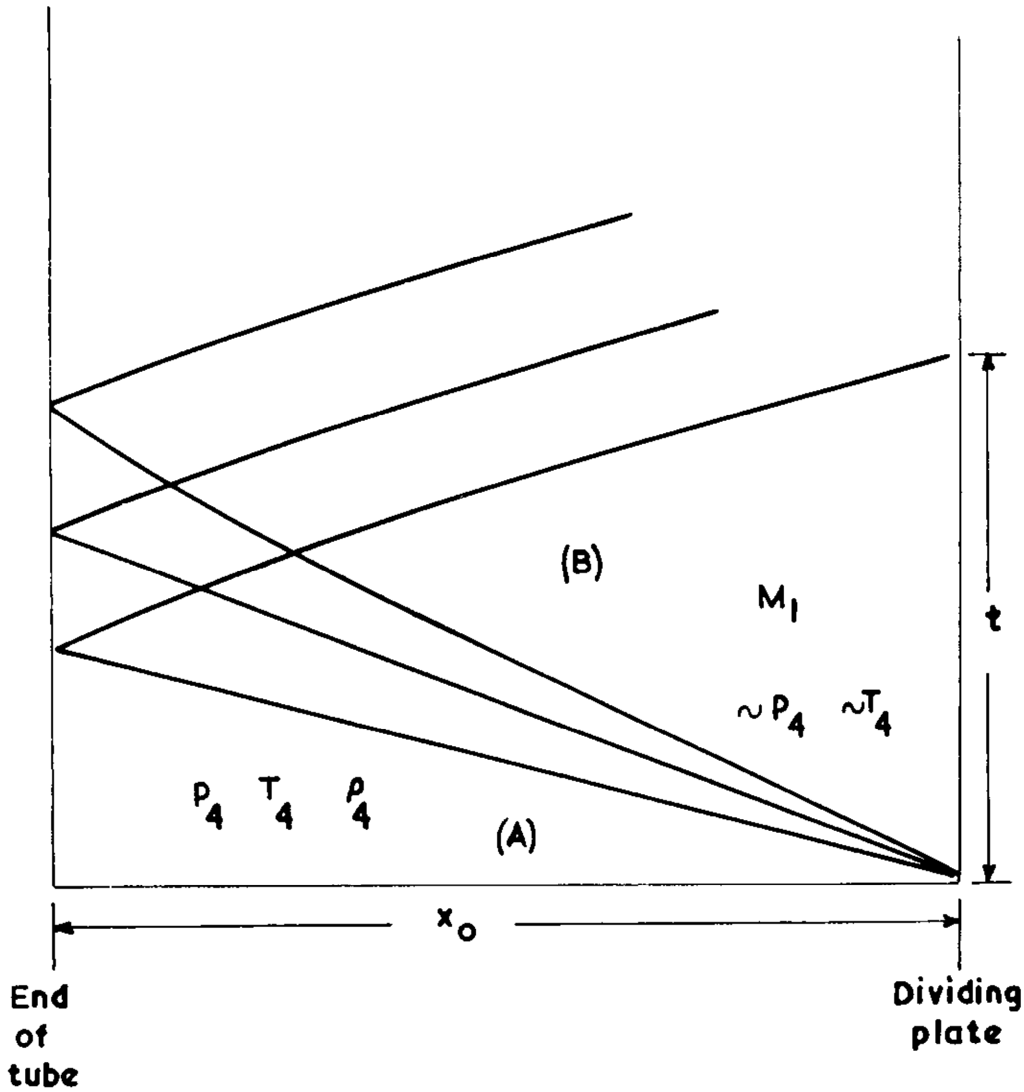

Flow in reservoir after expansion head has passed through hole in dividing plate.

Note that the pressure and temperature in regions (A) and (B) are assumed to be equal. This is approximately true in this case since $M_1 \approx 0{\cdot}06$.

FIG. 7

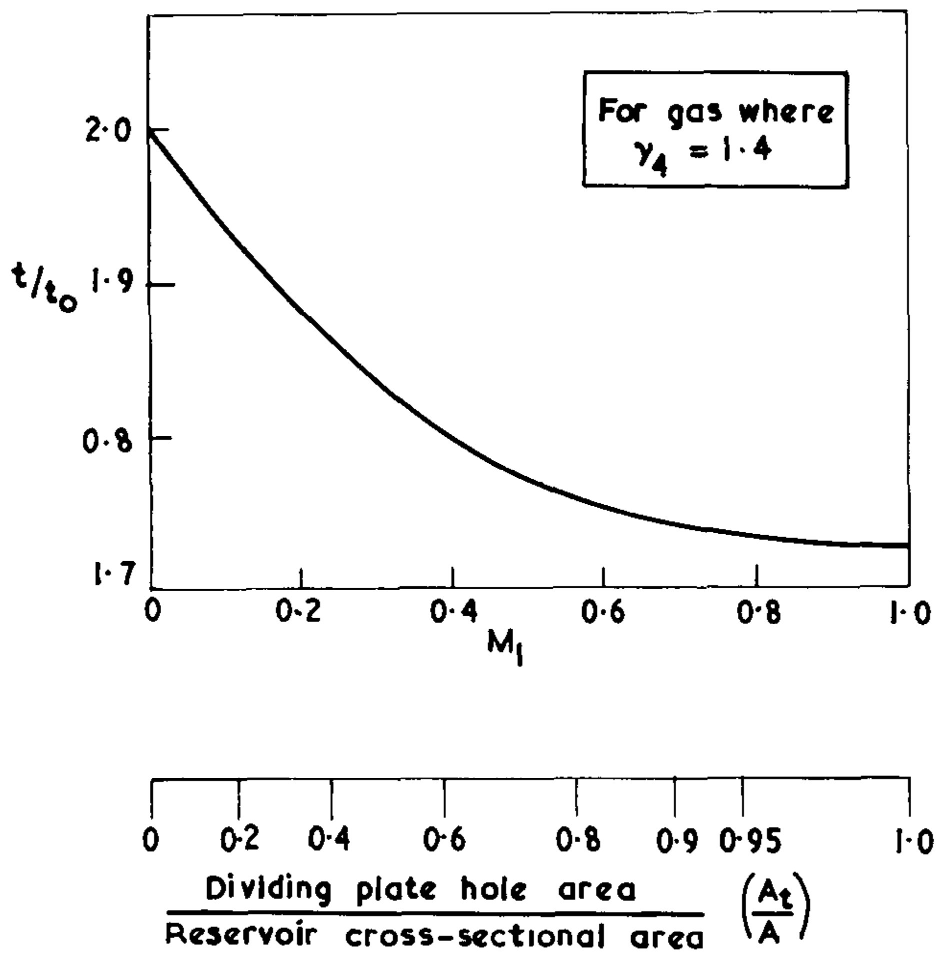

Time of constant flow through dividing plate hole before emergence of reflected expansion head.
(After Cable and Cox, Ref. 3.)

FIG. 8

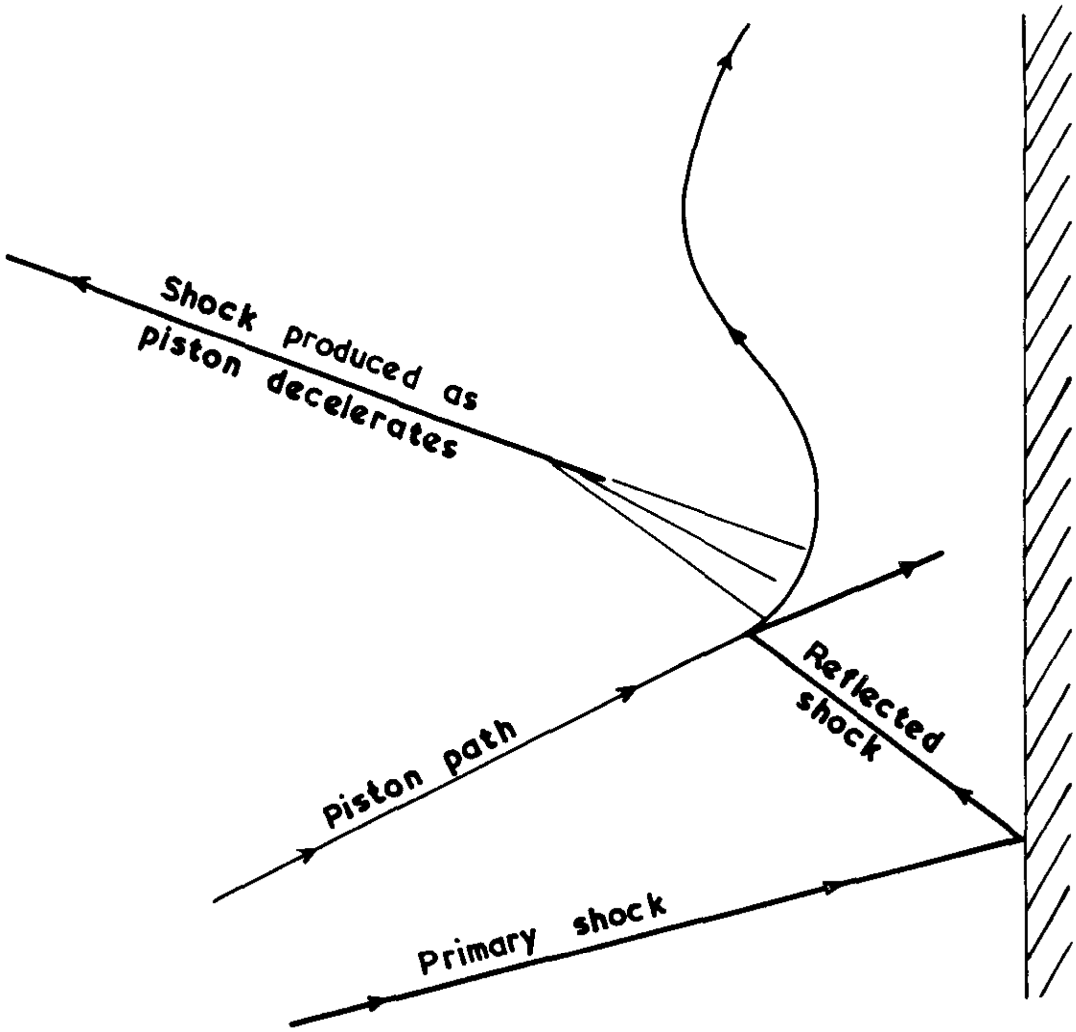

Shock produced by piston as it slows down at the end of the tube

28 957
FIG. 9

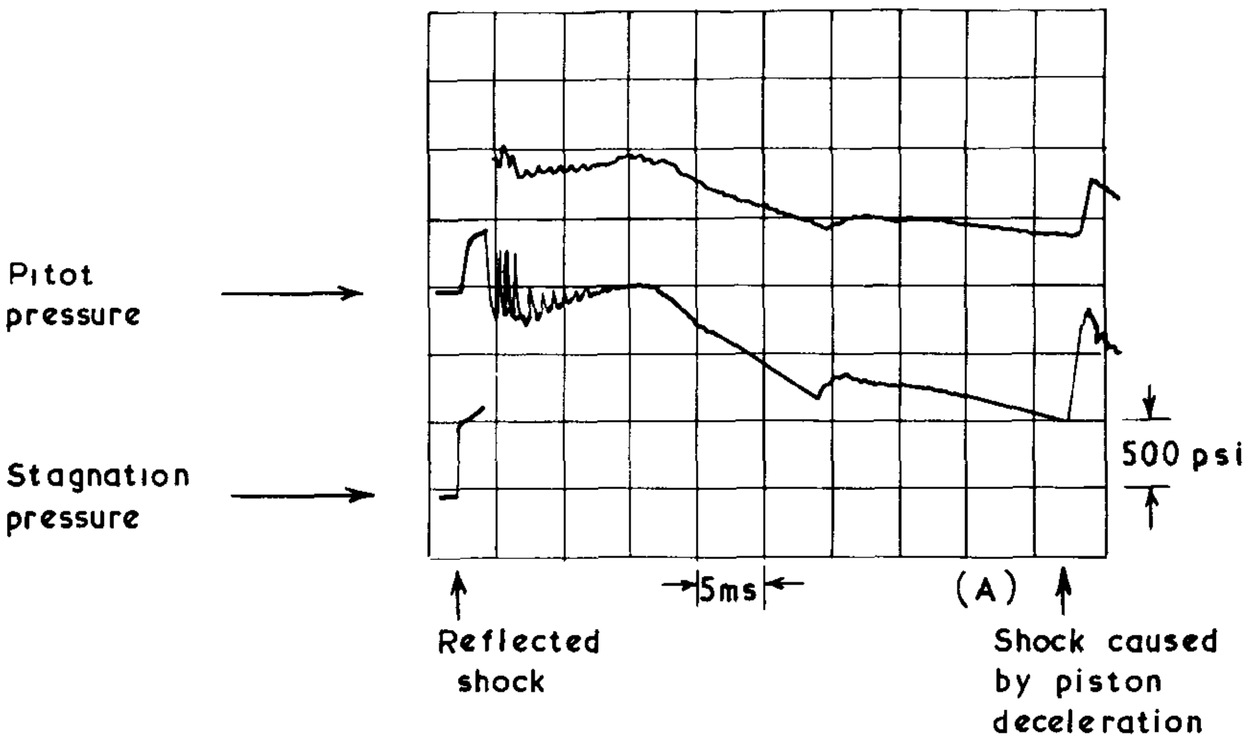

(a) Straight through driver — no driver reservoir

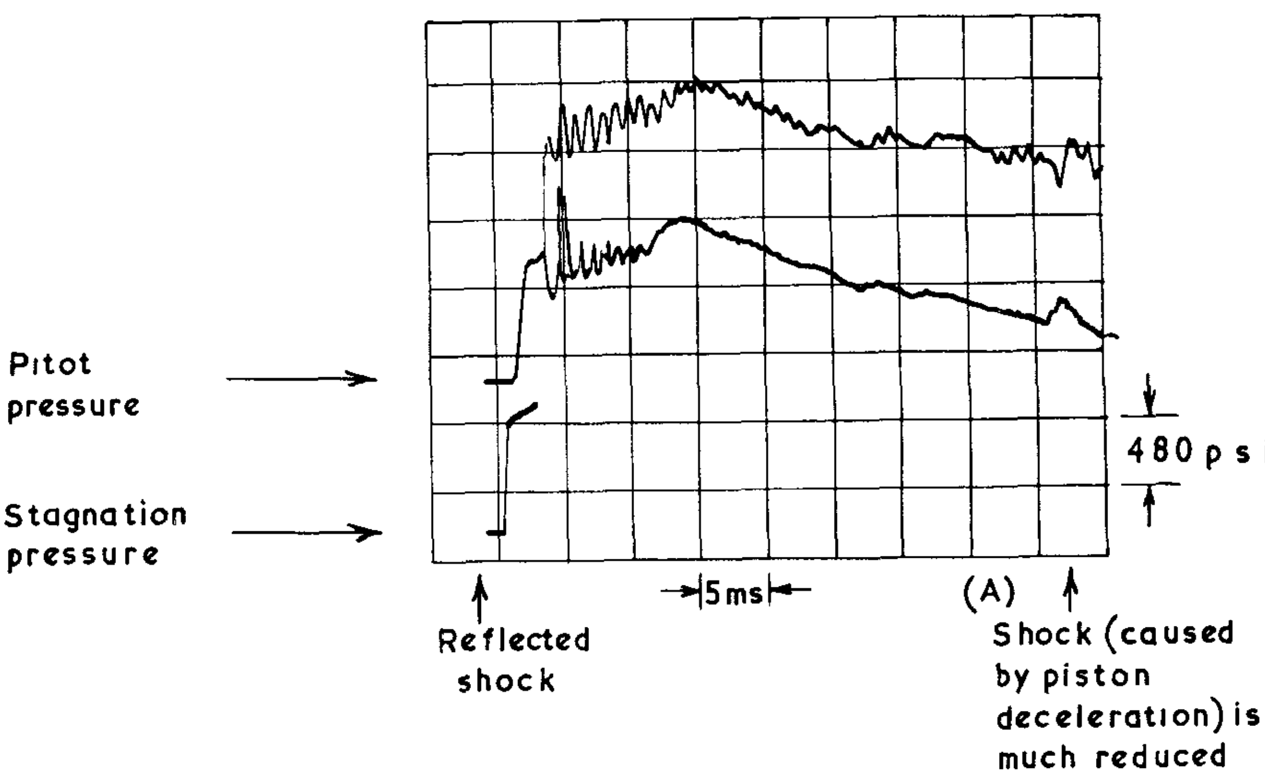

(b) Tunnel fitted with driver - reservoir

Pitot pressure and stagnation pressure traces showing reduction in strength of shock caused by the deceleration of the piston.

FIG. 10 (a & b)

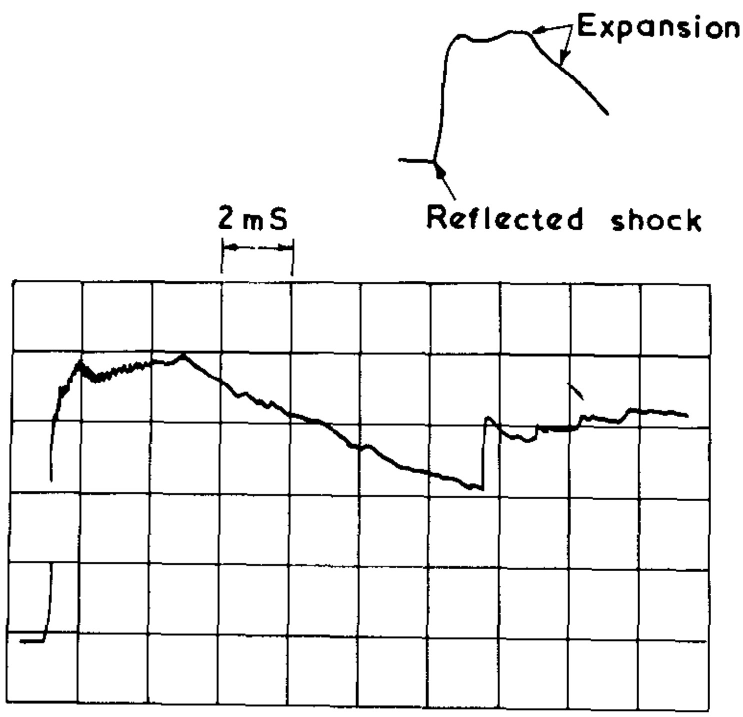

(a)

$P_4 = 1000$ lb/in.^{2}

He : N_2 $M_1 = 3{\cdot}6$

$\delta = 0{\cdot}316$

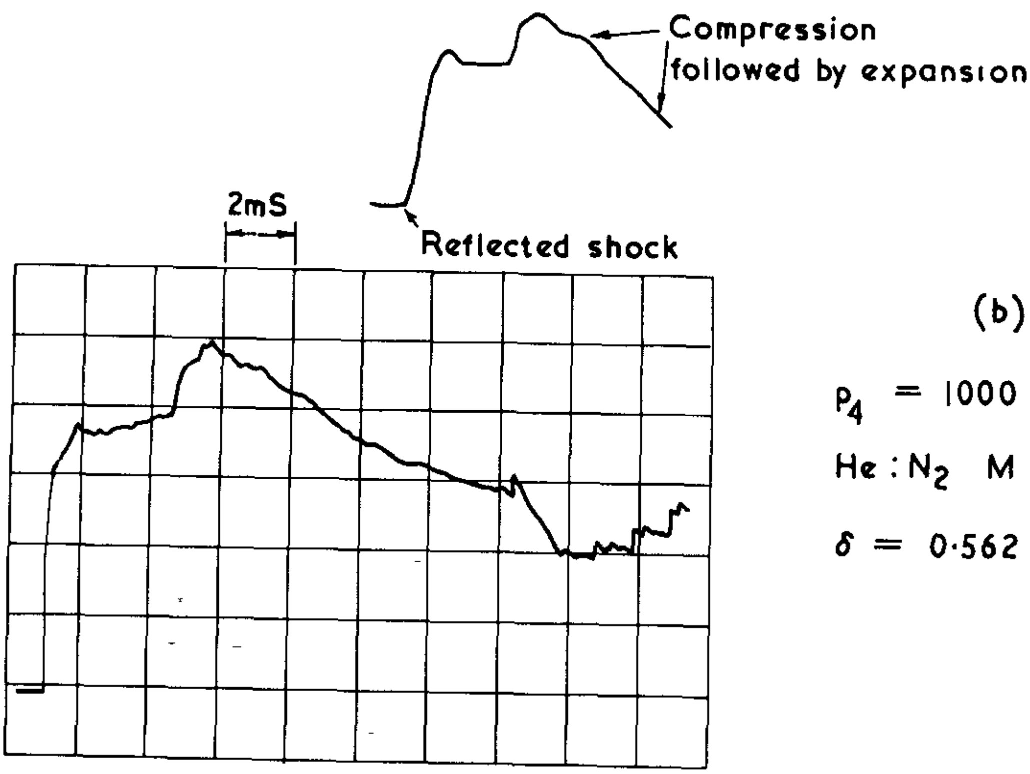

(b)

$P_4 = 1000$ lb/in.^{2}

He : N_2 $M = 3{\cdot}6$

$\delta = 0{\cdot}562$

Reflected-shock pressure records

FIG. 10 (c & d)

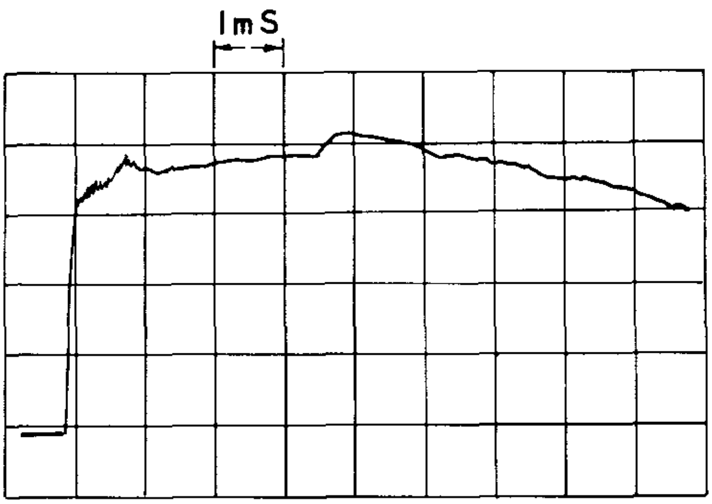

(c)

p_4 = 1 000 psi

He : N_2 M_1 = 3·6

δ = 0·380

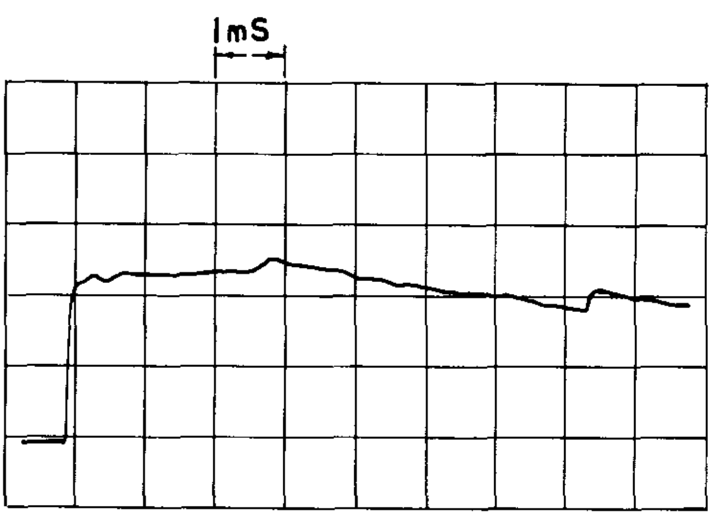

(d)

p_4 = 10 000 psi

He N_2 M = 3·73

δ = 0·380

Reflected – shock pressure records

FIG. 10 (e & f)

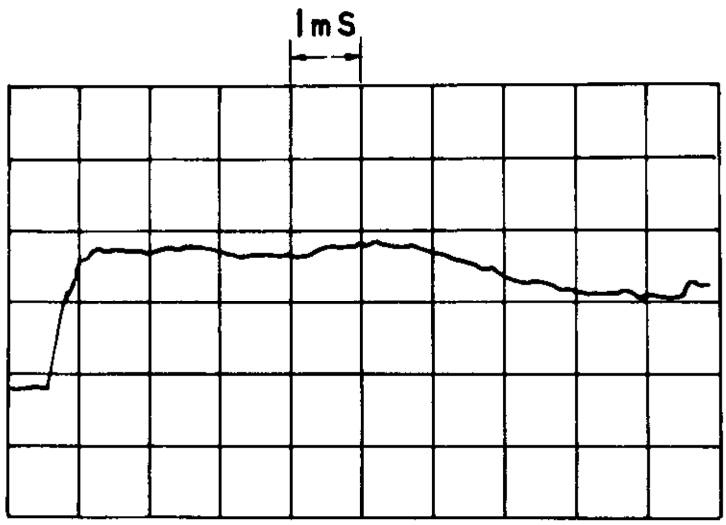

(e)

$p_4 = 1000$ psi

$He : N_2$ $M = 3{\cdot}6$

$\delta = 0{\cdot}38$

Working section flat plate heat transfer record $(He : N_2)$

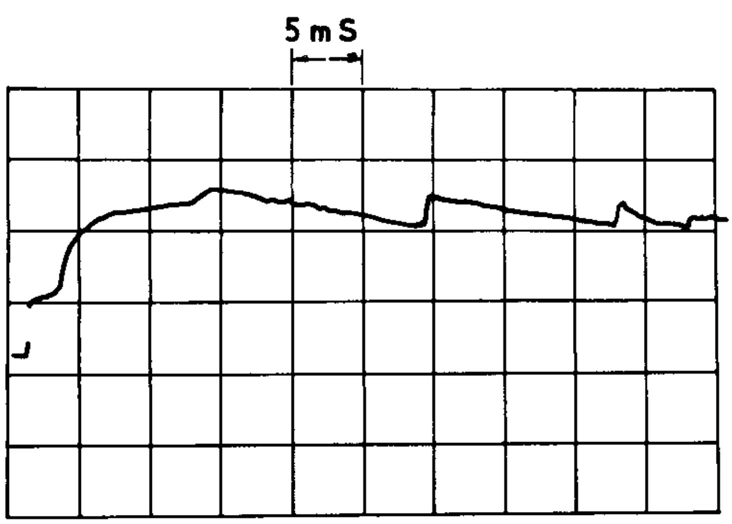

(f)

$p_4 = 2000\ lb/in.^2$

$N_2 : N_2$ $M_1 = 2$

$\sigma = 0\ 39$

Reflected – shock pressure record $(N_2 : N_2)$

FIG.10 g

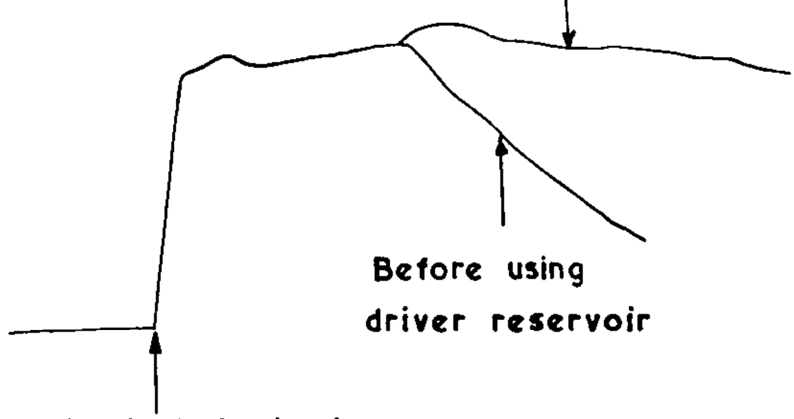

Comparison of pressure traces obtained before and after using the driver reservoir technique.
Helium as driver and nitrogen as driven gas.

Part 2 - Determination of Optimum Reservoir Size

By L. Davies,+ D. R. Brown*

and

G. Hooper*

List of Contents

---

1. Introduction

The driver-reservoir technique is employed in a shock tube, shock tunnel or gun-tunnel, when it is necessary to prevent the head of the expansion wave (see Fig. 1) reaching the end of the low pressure channel during the testing time. This is achieved by allowing the head of the expansion wave to interact with a perforated plate situated at the end of the high pressure chamber. This perforated plate separates the driver from a large volume vessel known as the reservoir (see Fig. 2). By adjusting the size of the holes, or hole, in the perforated plate, a matching condition can be found such that only a Mach wave is propagated downstream. By this means an increase in running time of three or four times was demonstrated by Henshall et al[1], who devised the technique.

The purpose of the reservoir is to ensure that the flow through the perforated plate (referred to throughout the paper as the orifice plate) after passage of the expansion wave, is not interrupted during the running time. In this respect the dimensions of the reservoir are most important.

In/

+ National Physical Laboratory.

* University College of Wales, Aberystwyth.

In this paper the factors which determine the choice of reservoir dimensions are discussed, and the method of finding the optimum reservoir size for a particular facility is given. The experiments which formed part of this investigation are described, and include a study of the flow within the reservoir.

2. Determination of the Hole Size in the Orifice Plate

Unless otherwise stated it will be assumed throughout this paper that there is only one hole central in the orifice plate. A detailed experimental study of the determination of the hole size necessary to eliminate the reflected head of the expansion wave has been described by Henshall et al[1], and Davies and Dolman[2]. A theoretical study has been carried out by Flagg[3], who only considers the interaction of the expansion wave with the perforated plate. From this work the ratio of hole area to driver cross-section area which is required to eliminate the reflected head of the expansion wave is found to be given by the equation[3].

$$\delta = \left(\frac{\gamma_4 + 1}{2}\right)^{\frac{(\gamma_4 + 1)}{2(\gamma_4 - 1)}} \frac{U_{3S}}{a_4} \left[1 - \frac{\gamma_4 + 1}{2}\left(\frac{U_{3S}}{a_4}\right)^2\right]^{\frac{1}{(\gamma_4 - 1)}} \quad \ldots (1)$$

where $\delta = A_t/A_d$.

δ is obtained from equation 1 using the following relationships:

$$\frac{U_{3U}}{a_4} = \frac{2}{a_{41}\,(\gamma_1 + 1)}\left(M_{ST} - \frac{1}{M_{ST}}\right)$$

where M_{ST} is the Tailored primary shock Mach number.

$$\frac{p_{3U}}{p_4} = \left(1 - \frac{(\gamma_4 - 1)}{2} \cdot \frac{U_{3U}}{a_4}\right)^{\frac{2\gamma_4}{\gamma_4 - 1}}$$

$$\frac{U_{3S} - U_{3U}}{a_4}\left(\frac{a_4}{a_S}\right) = \left[\frac{2}{\gamma_4(\gamma_4 - 1)}\right]^{\frac{1}{2}} \frac{\frac{p_{3U}\,p_4}{p_4\,p_{3S}} - 1}{\left[1 + \left(\frac{\gamma_4 + 1}{\gamma_4 - 1}\right) \cdot \frac{p_{3U}}{p_4} \cdot \frac{p_4}{p_{3S}}\right]^{\frac{1}{2}}}$$

$$\frac{a_3}{a_4} = \left[1 - \frac{(\gamma_4 - 1)}{2}\left(\frac{U_{3S}}{a_4}\right)^2\right]^{\frac{1}{2}}$$

The values calculated for δ are intended to serve as a guide, and the practical value must be determined experimentally. In the present study a shock tube 14 ft long (4·27 m), made of wave guide 2 in. × 1 in. (5·08 cm × 2·54 cm), was used. The test section was 10 ft (3 m) long and the driver section

4 ft/

4 ft (1·22 m) long. In this tube when air was used as both driver and test gas at a primary shock Mach number of 2, the experimental value of δ was found to be 0·383 as compared with 0·379 predicted by equation (1). When helium was used as driver gas and air as test gas, then the experimental value of δ was found to be 0·32.

The evaluation of δ when Mach numbers other than the tailoring value are used, is discussed in Refs. 1 and 2.

3. Determination of the Optimum Reservoir Size

Henshall et al have shown that the reservoir volume must be large enough to ensure that the pressure within the reservoir does not fall significantly during the running time. An analysis of the flow within the reservoir has been suggested in Ref. 2 following an argument outlined in Ref. 4.

The essential points are as follows:

Just after the main diaphragm bursts, the head of the expansion wave (see Fig. 1) interacts with the orifice plate. Part of the expansion wave passes through the hole in the plate and into the reservoir. The strength of this transmitted wave is a function of (A_t/A_r). This wave reflects from the end of the reservoir and on reaching the orifice plate, it will reflect as from a closed end if the ratio A_t/A_r is very small. A weak transmitted wave propagates downstream through the orifice plate. The relationship between the strength of this transmitted wave and the ratio A_t/A_r is to be determined so that the conditions at the end of the low pressure section will not be significantly affected during the running time.

A simple theoretical approach to this problem is to assume that the expansion wave which passes into the reservoir at the start of the run is a single concentrated wave. This follows the Ludweig tube analysis of Cable and Cox[4]. These authors suggest that if the ratio A_t/A_r is very small, then the flow Mach number behind the expansion fan is small, and thus the width of the fan is small compared to the length of the reservoir. The assumption of a single concentrated wave is then a good approximation for the first few reflections. It is thus possible to think in terms of reflections of this single wave at the ends of the reservoir.

In the present case this is not a particularly realistic description of the flow within the reservoir, but the agreement with experiment warrants its use as a first approximation. It is found, in fact, that pressure within the reservoir falls initially in a series of discrete steps (see Fig. 2b), which is in accord with the simple theory. The time between these steps also agrees closely with the theoretical times.

In terms of this model, the length of the reservoir will then determine the number of reflections of the expansion within the reservoir during the running time. This in turn decides the rate of fall in pressure. The task is to determine the optimum reservoir cross section, which controls the strength of the wave, and then to determine the optimum reservoir length.

The pressure (p_n) at the orifice plate end of the reservoir after the n th. reflection of the expansion wave at that end is given by the equation:

p_n/

$$\frac{p_n}{p_4} = \left\{\frac{1 - \frac{(\gamma_4 - 1)}{2} M_1}{1 + \frac{(\gamma_4 - 1)}{2} M_1}\right\}^{\frac{2\gamma_4(n-1)}{\gamma_4 - 1}} \frac{1}{\left\{1 + \frac{(\gamma_4 - 1)}{2} M_1\right\}^{2\gamma_4/(\gamma_4 - 1)}} \qquad \ldots (2)$$

where p_4 is the initial reservoir pressure and M_1 is the flow Mach number behind the expansion wave, following its first entry into the reservoir via the orifice plate. M_1 is obtained from the equation

$$\frac{A_r}{A_t} = \frac{1}{M_1} \left\{\frac{1 + \frac{(\gamma_4 - 1)}{2} M_1^2}{\frac{\gamma_4 + 1}{2}}\right\}^{(\gamma_4 + 1)/\{2(\gamma_4 - 1)\}}$$

Curves of p_n/p_4 versus n for various A_r/A_t are shown in Fig. 3a for air and Fig. 3b for helium. The maximum allowable fall in pressure is to 85% of the initial pressure. This value was examined empirically, and the 85% line is therefore used to assess the effect of A_r/A_t ratios. Above a particular value of A_r/A_t the gain is small. For air this value is about 100, and from the engineering aspect, this is the optimum cross section since the strength of the expansion wave is not significantly reduced for larger values. (See Fig. 4a). In Fig. 4a the pressure after an arbitrarily chosen 12 reflections of the wave is plotted as a function of A_r/A_t . The time taken for the wave to travel from the orifice plate to the end of the reservoir and back is given by equation (3).

$$\frac{t}{t_0} = \frac{2}{(1 + M_1)} \left\{1 + \frac{(\gamma_4 - 1)}{2} M_1\right\}^{(\gamma_4 + 1)/\{2(\gamma_4 - 1)\}} \qquad \ldots (3)$$

where t_0 is the time taken for a disturbance travelling at the initial speed of sound to travel the length of the reservoir assuming the gas to be at rest.

The time taken for the n+1 reflection is

$$\frac{t_{n+1}}{t_0} = \frac{2}{1 + M_1} \left\{1 + \frac{(\gamma_4 - 1)}{2} M_1\right\}^{\frac{\gamma_4 + 1}{2(\gamma_4 - 1)}} \left\{\frac{1 + \frac{(\gamma_4 - 1)}{2} M_1}{1 - \frac{(\gamma - 1)}{2} M_1}\right\}$$

If the pressure fall in the reservoir, after a given time, is examined as a function of reservoir length, it is clear from Fig. 4b that after 12 in. (30 cm) there is no significant gain from increasing the length. 12 in. is

therefore/

therefore about the optimum value in the present case. The "given time" is the time it takes for the reflected shock to travel up the tube and back. In the absence of the expansion wave head, this process will limit the running time at the end plate. Clearly, the time involved will depend on the length of the driver and test sections and as a rough guide may be considered to vary linearly with these lengths. The optimum reservoir length will therefore vary in a similar manner.

The length of the reservoir and its cross-sectional area are determined separately, for physically realistic conditions. Clearly, any A_r/A_t will do if the length is infinite, and conversely length will not matter if A_r/A_t is infinite. The reason for using the driver-reservoir technique, however, is to obtain a large increase in running time without having to resort to using very long driver sections. This immediately limits the length of the driver-reservoir, i.e. it must not be much longer than the original driver section. Secondly, from the constructional aspect there is no reason for going to a larger reservoir than necessary especially if high pressure operation is anticipated. This sets an upper limit to the area.

The area of the hole in the orifice plate is determined independently of the reservoir dimensions, since the elimination of the reflected expansion head is effected solely by the interaction of the expansion wave head with the orifice plate.

4. Experimental Investigation

For the experiments where air was used as driver gas, the primary shock Mach number was arbitrarily chosen as 2, whereas for helium as driver gas the tailoring Mach number, 3·4, was used. The principles involved will however apply at other Mach numbers than these. In all cases air was used as test gas.

Determination of correct orifice plate hole size

The determination of the correct orifice plate hole size was carried out as outlined in Refs. 1 and 2. The results for both driver gases are shown in Figs. 5a, b, c and d. In Fig. 5a the sketch of the reflected shock pressure-time profile indicates the important features. The pressure at the end of the shock tube first rises to a value which, in the air case, is the equilibrium interface value (p_e), and in the helium driver case will be the reflected shock pressure p_5. With the end of the driver section blocked (or nearly so), a strong expansion wave reaches the end plate and terminates the running time. This is labelled in the sketch as "hole too small", and the lower bound is where $\delta = 0$. For increasing values of δ the strength of the expansion wave decreases. The "hole too large" line refers to the condition when the orifice plate hole is larger than ideal and a compression wave results. h_1 is shown on the sketch as referring to values greater than p_e (or p_5) and it is also used to indicate the deviation for smaller pressures. Therefore, if an expansion wave occurs (h_1/h_2) is plotted as a negative value, and if a compression wave occurs (h_1/h_2) is plotted as a positive value. In this way it is possible, by drawing a line through the series of points produced, to obtain the ideal (A_t/A_d) as an intercept on the δ axis. For this value of δ only a Mach wave is produced when the expansion head interacts with the orifice plate.

The pressure traces for air are shown in Fig. 5c. The two extreme δ cases, i.e. unity and 0, and the ideal case are demonstrated. Similarly, the pressure records for helium are shown in Fig. 5d.

Determination/

Determination of optimum reservoir cross-sectional area

It has been shown in Section 3 that the theoretical optimum length for air as driver gas is about 12 in. This length was therefore used for most of the reservoirs since, as discussed in the cross section, the optimum A_r/A_t is obtained independent of the length. The various reservoir dimensions, together with their identifying numbers, are given in Table 1.

TABLE 1

Reservoir number	area (in²)	A_r/A_t	length
0	1·627	2·164	12 in.
1	6·56	10·541	12 in.
2	29·6	47·56	12 in.
3	66·6	107·2	12 in.
3a	66·6	107·2	6 in.
3b	66·6	107·2	24 in.
4	123·2	197·9	12 in.
5	139·2	223·68	12 in.
6	153·9	247·3	12 in.

An indication that the area ratio of a particular reservoir is below the minimum allowable value is that the pressure p_e starts to fall away significantly before the end of the running time. This is demonstrated in Fig. 6. In the sketch at the top of the page the essential features are indicated. p_{ef} is the final value of p_e before the arrival of the shock wave which terminates the running time.

As regards the pressure traces, that for reservoir 1 shows that even though the correct orifice plate is used, there is still an expansion wave travelling down the tube. Clearly, this is due to the fact that expansion waves from within the reservoir which are transmitted downstream through the hole in the orifice plate are too strong, as predicted by the theory. For reservoir 2 the expansion wave is not as strong, and from reservoir 3 on (i.e. increasing area ratio), there is no significant fall in pressure and no significant improvement. Reservoir 3 is therefore the one with the optimum area ratio (i.e. ~ 100).

The helium driver case is also demonstrated in Fig.6. Here the optimum area ratio is not reached until reservoir 6 is used. (Area ratio ~ 250).

Determination of optimum reservoir length

Some tests on the effect of reservoir length were carried out with air as driver gas and using the optimum area ratio. Three reservoirs were used, numbers 3, 3a and 3b. From Table 1 it can be seen that their lengths bear a simple relation to one another.

In/

In Fig. 7 the top trace is for reservoir 3a (L = 6 in., 15 cm) and here there is a significant fall away in pressure before the end of the running time. In the bottom trace, for reservoir 3b (L = 24 in., 61 cm) there is no significant improvement over the trace obtained for reservoir 3 (L = 12 in., 30 cm) and which is shown in Fig. 6. This indicates that for these conditions 12 in. (30 cm) is about the optimum length and bears out the theoretical prediction.

Examination of the pressure-time variation in the reservoir

The variation of the pressure in the reservoir was examined using the pressure gauge station shown in Fig. 2. In Figs 8a, b, c, d the experimental and theoretical pressure-time variations are compared for different reservoirs and for helium and air as driver gases. In Fig. 8a the variation in reservoirs 3, 3a and 3b (increasing length) for air are shown. In Fig. 8b the pressure-time variations in reservoirs 1, 2 and 5 (increasing area) are shown, also for air. It is seen that the theoretical curves indicate the actual trends reasonably well considering the simplifying assumptions used in the theoretical model (see Ref. 4). In the helium cases shown in Figs 8c and 8d the agreement between experiment and theory is not good. It is some consolation, however, that the theory is too pessimistic in predicting the fall in reservoir pressure with time, and this suggests that the actual optimum area ratio will be less than the theoretical. This will be of use when constructing a driver-reservoir system.

The increase in running time obtained using the driver-reservoir technique

By eliminating the reflected head of the expansion wave an increase of four times the original testing time was obtained by Henshall et al[1] , using hydrogen as driver gas and air as test gas. In the present investigation the increase for air as driver and test gas was three times the original, and using helium the increase was four times, in accordance with the results in Ref.1.

5. Conclusions

The following conclusions are drawn from this investigation:

1. For most efficient use of the driver-reservoir technique there is an optimum reservoir size which depends on the shock-tube dimensions and the initial conditions.

2. The optimum cross-sectional area is determined by the strength of the expansion wave which is transmitted through the orifice plate into the reservoir. The strength of this wave in the reservoir is a function of the ratio of the orifice plate hole to the reservoir area. The maximum allowable strength thus determines the optimum area.

3. The optimum length of the reservoir is obtained by ensuring that the fall in reservoir pressure will not cause a significant drop in pressure at the end of the low pressure channel during the testing time.

4. The fall in pressure in the reservoir and the strength of expansion waves transmitted through the orifice plate into the shock tube will then have no significant effect on the flow in the tu e during the testing time.

5. The method of determining the correct orifice plate hole size[1,2,3], and optimum reservoir dimensions are described in this paper, and it is shown that the optimum driver cross-sectional area is independent of the length.

6. Using the driver-reservoir technique an increase in testing time of three to four times may be obtained in a simple shock tube.

Nomenclature

A	Cross-sectional area
A_d	Driver cross-sectional area
A_t	Driver cross-sectional area of orifice plate hole
A_r	Reservoir cross-sectional area
a	Sound speed
a_i	Sound speed in region i
M	Mach number
M_S	Mach number of primary shock
M_i	Mach number in region i
p_i	Pressure in region i
P_{ij}	p_i/p_j
t	Time
t_o	Time taken for a disturbance travelling at speed of sound to travel the length of the reservoir assuming the gas to be at rest
U_i	Velocity in region i
U_{iS}	Velocity in region i due to steady gas expansion
U_{iU}	Velocity in region i due to unsteady gas expansion
γ_i	Ratio of specific heats in region ν
δ	A_t/A_d

Subscripts

1,2,3...	Refer to regions shown in Fig. 1 unless otherwise stated.

References/

References

No.	Author(s)	Title, etc.
1	B. D. Henshall, R. N. Teng and A. D. Wood	Development of very high enthalpy shock tunnels with extended steady state test times. AVCO Tech.Rep.RAD-TR-62-1, 6. 1962.
2	L. Davies and K. Dolman	On the driver-reservoir technique in shock and gun tunnels. NPL Aero Report 1226. A.R.C.28 957. 1967.
3	R. F. Flagg	A theoretical analysis of the driver-reservoir method of driving hypersonic shock tunnels. UTIAS Tech.Note No. 93. 1965.
4	A. J. Cable and R. N. Cox	The Ludwieg pressure-tube supersonic wind tunnel. Aeron.Quart., Vol.XIV. 1963

BMG

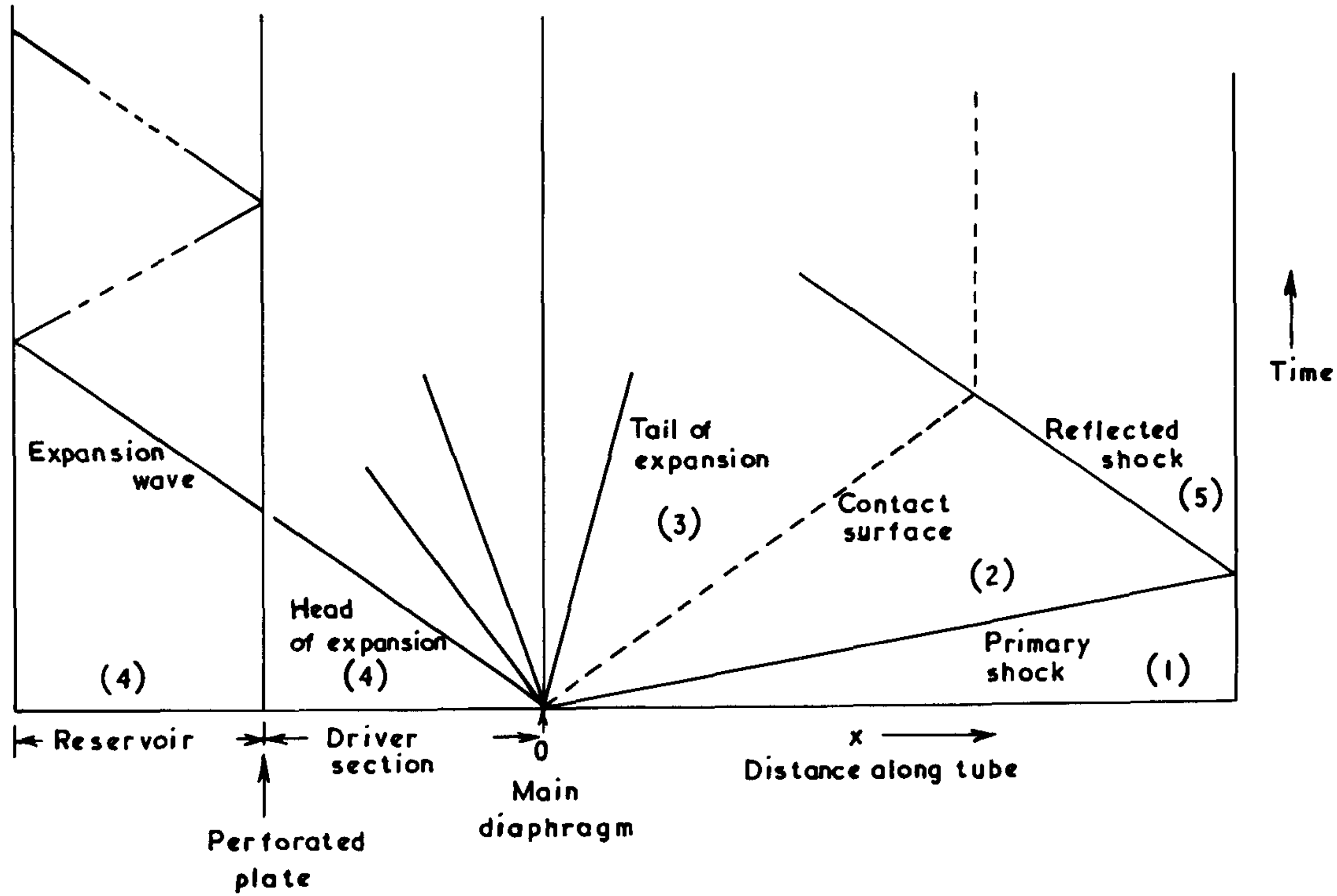

FIG. 1

Flow in shock-tube using driver-reservoir technique

FIG 2 a

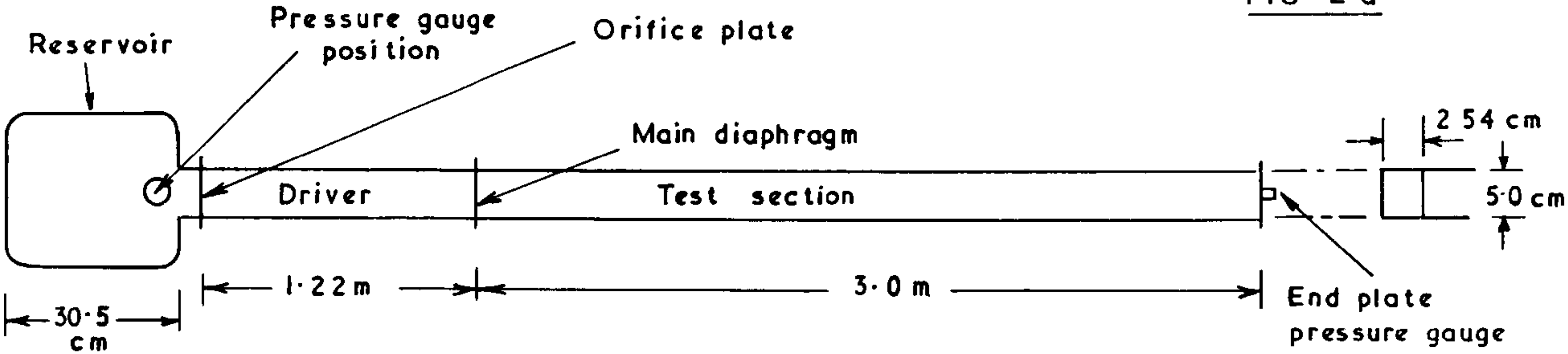

Experimental layout

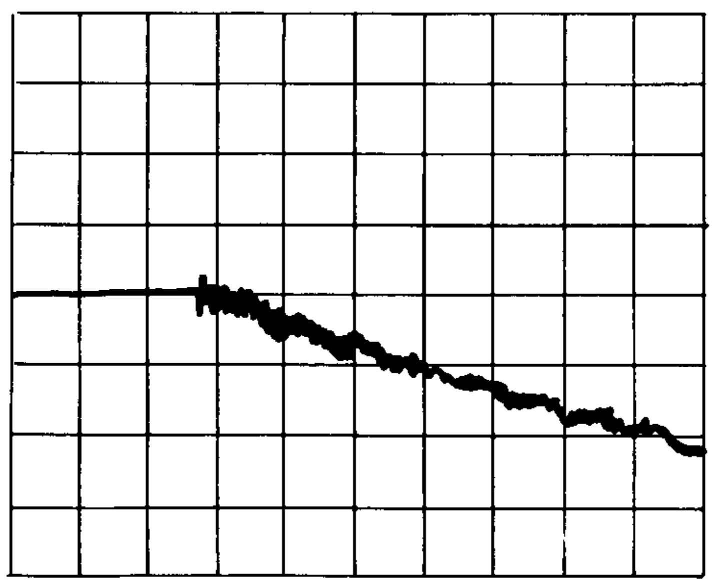

FIG. 2 b

Pressure time variation within reservoir 2 $A_r / A_t = 47{\cdot}56$ showing the pressure falling in discrete steps. Test gas Air

FIG 2(a & b)

FIG 5a

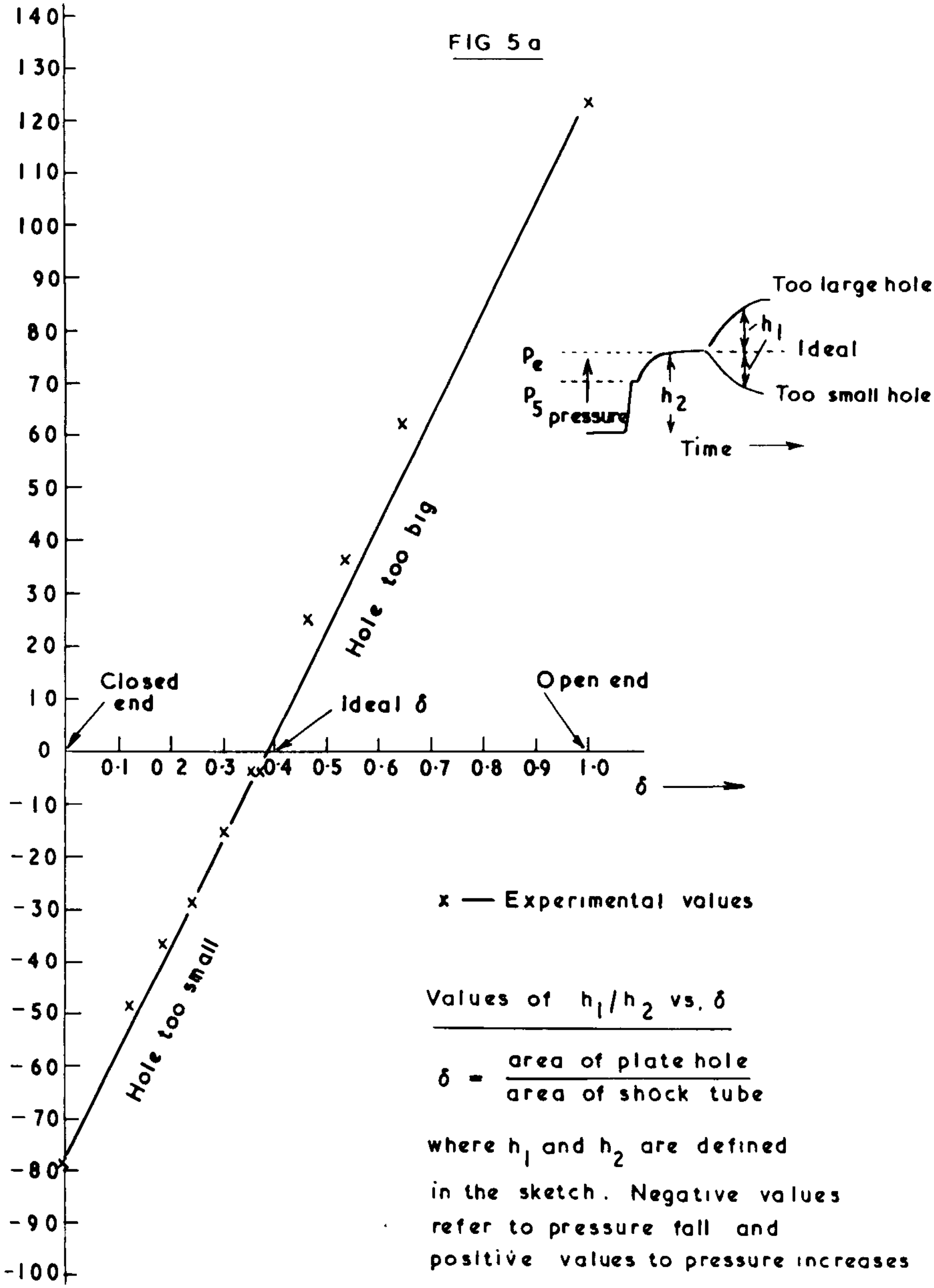

Values of h_1/h_2 vs. δ

$$\delta = \frac{\text{area of plate hole}}{\text{area of shock tube}}$$

where h_1 and h_2 are defined in the sketch. Negative values refer to pressure fall and positive values to pressure increases

Air as driver gas

FIG. 3 b

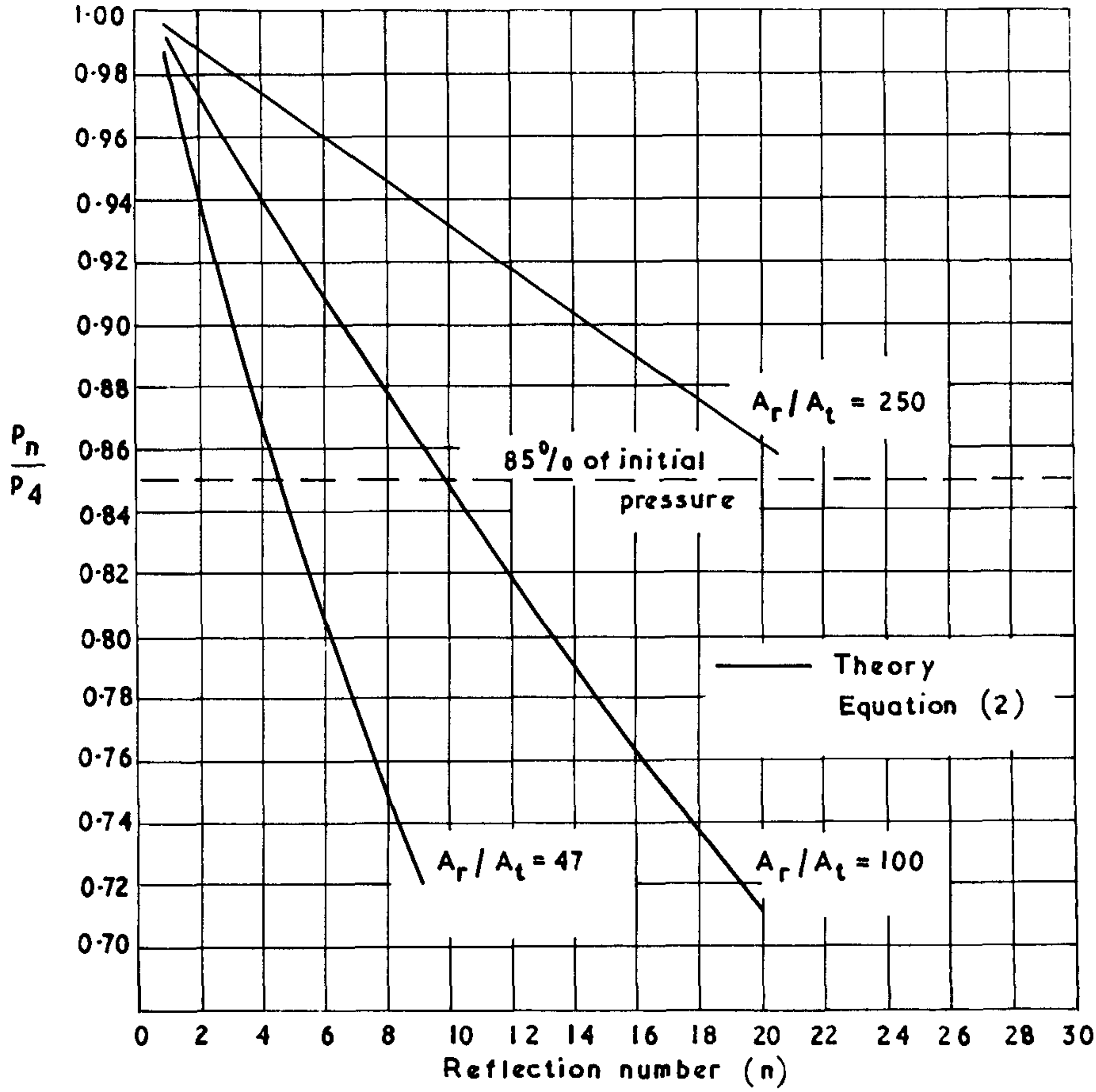

Pressure in reservoir after n reflections, normalised with respect to p_4, versus reflection number

FIG. 4(a) & (b)

FIG 4(a)

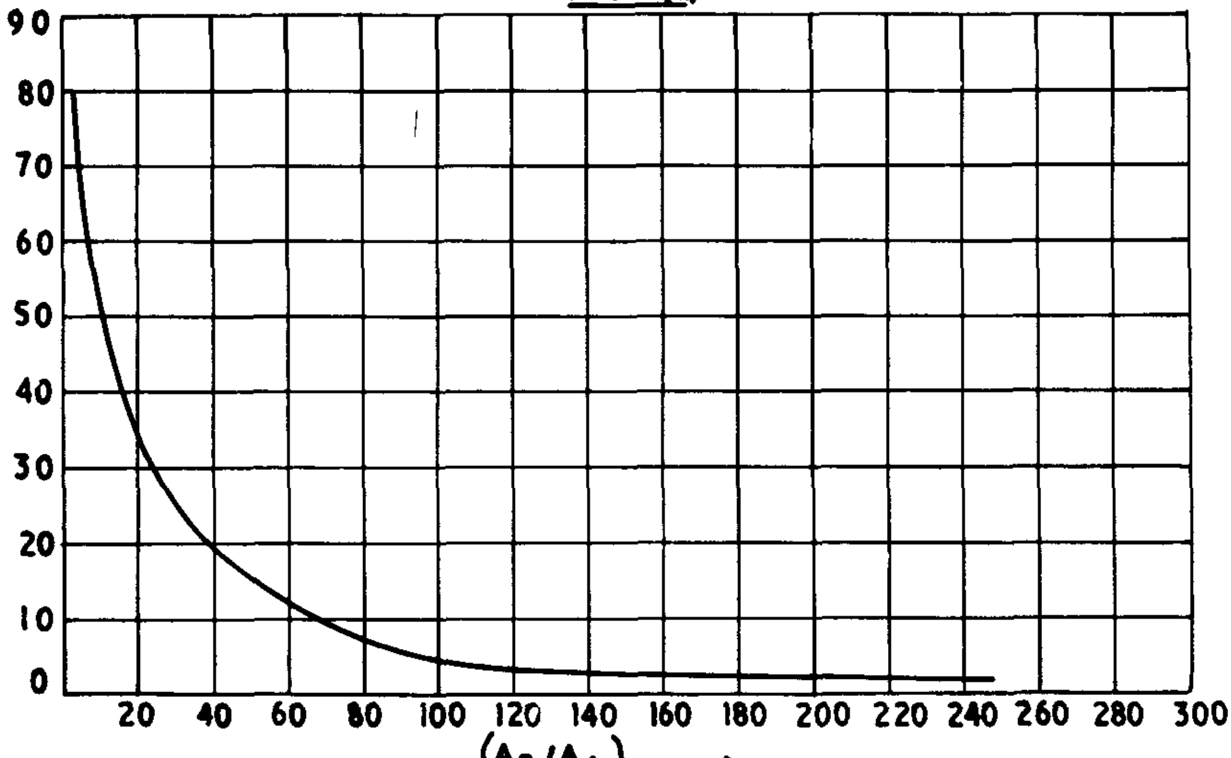

Pressure ratio after 12th reflection versus area ratio

FIG. 4(b)

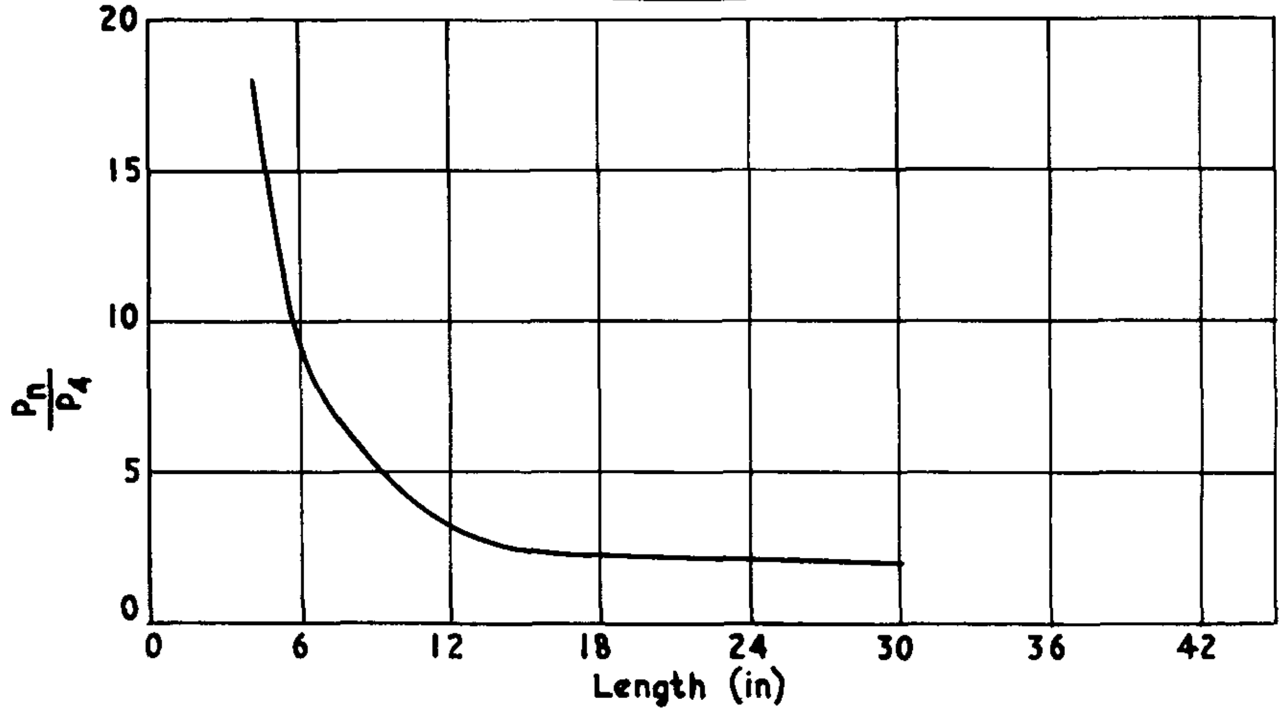

Pressure after give time versus reservoir length, where A_r/A_t = 107 initial pressure, p_4

FIG 5a

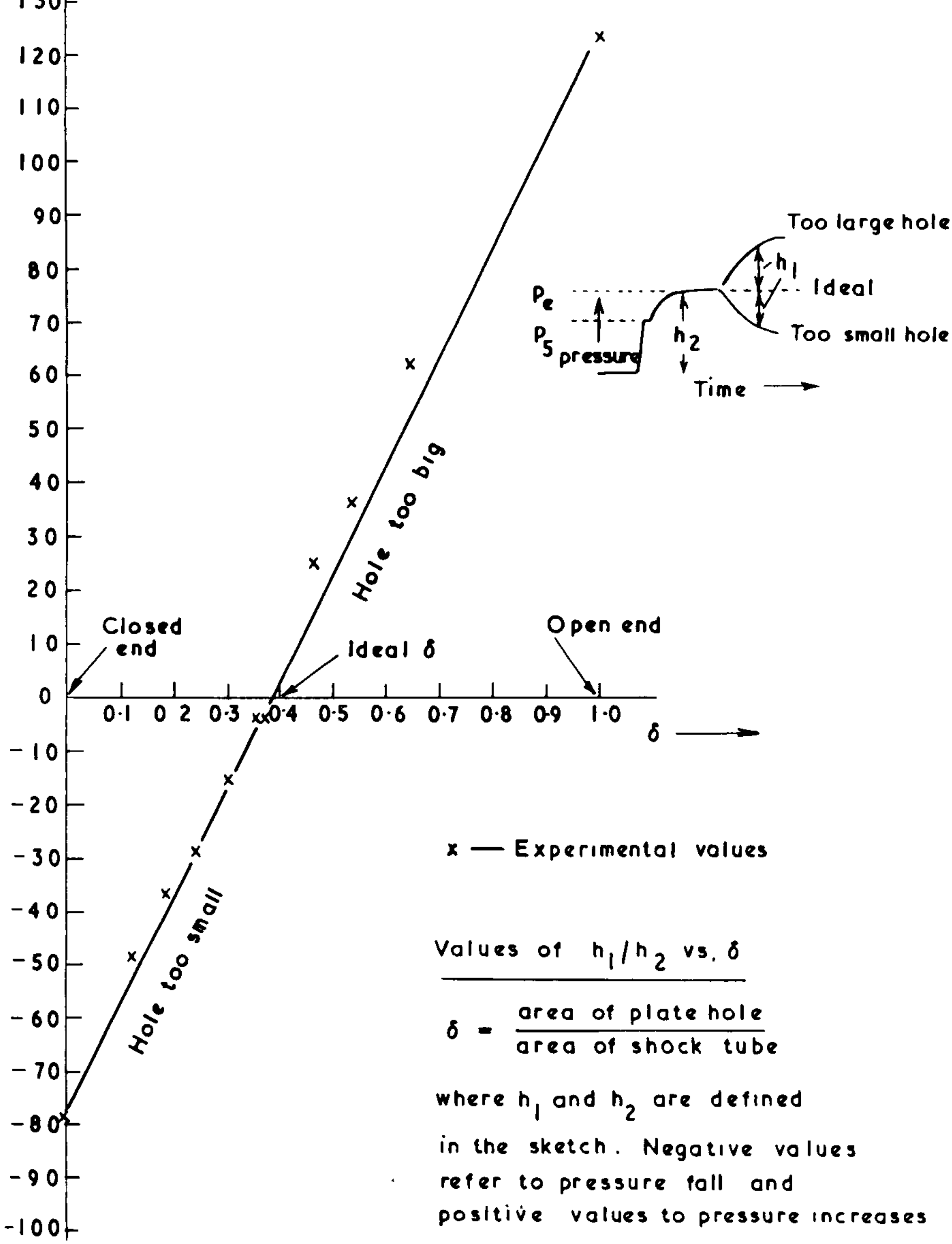

Values of h_1/h_2 vs. δ

$$\delta = \frac{\text{area of plate hole}}{\text{area of shock tube}}$$

where h_1 and h_2 are defined in the sketch. Negative values refer to pressure fall and positive values to pressure increases

Air as driver gas

FIG 5 b

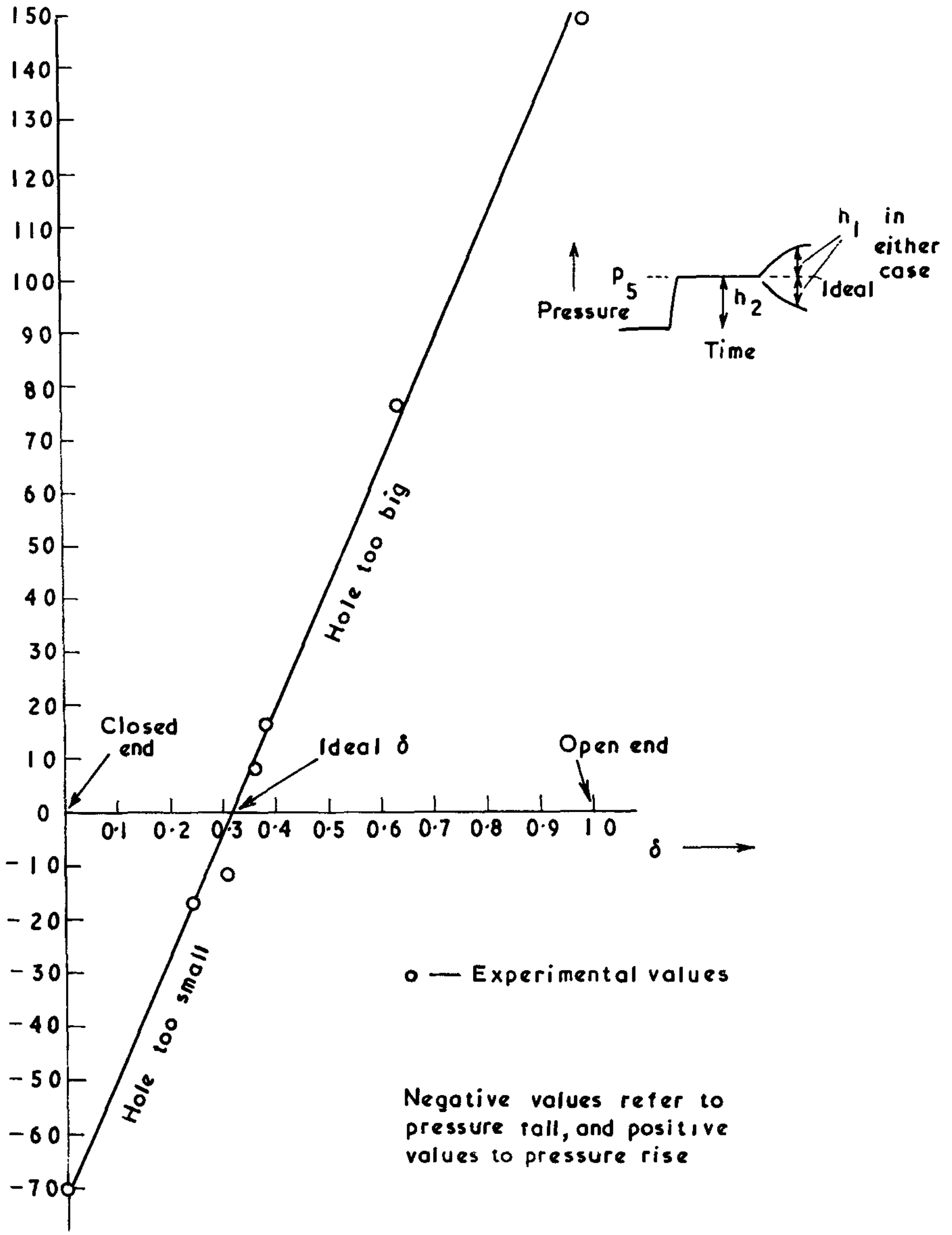

Values of h_1/h_2 vs δ (Helium)

FIG 5.c

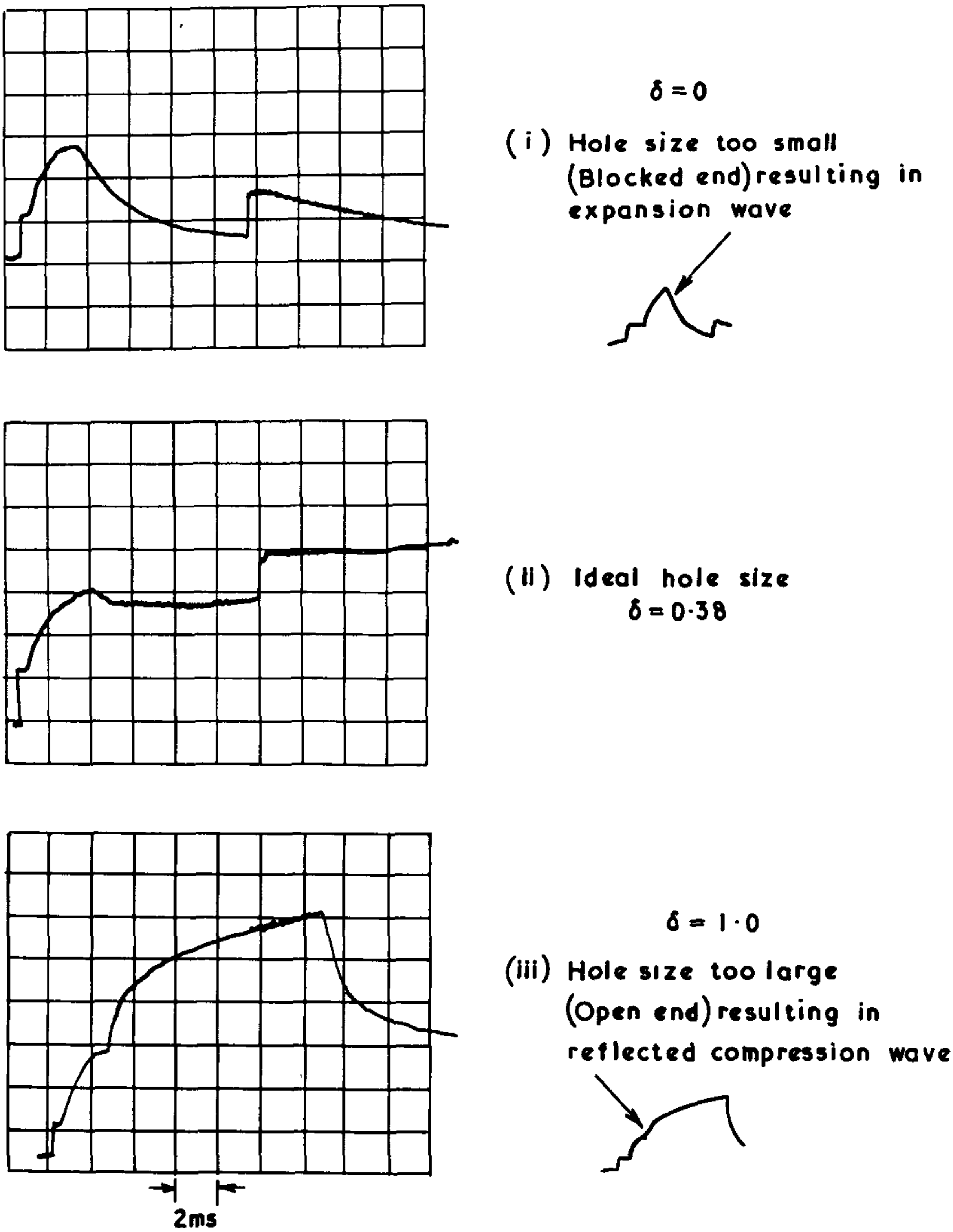

Air as driver gas. $M_s = 2$, P_4 = atm. pressure. 5 m secs per division time base

FIG. 5d

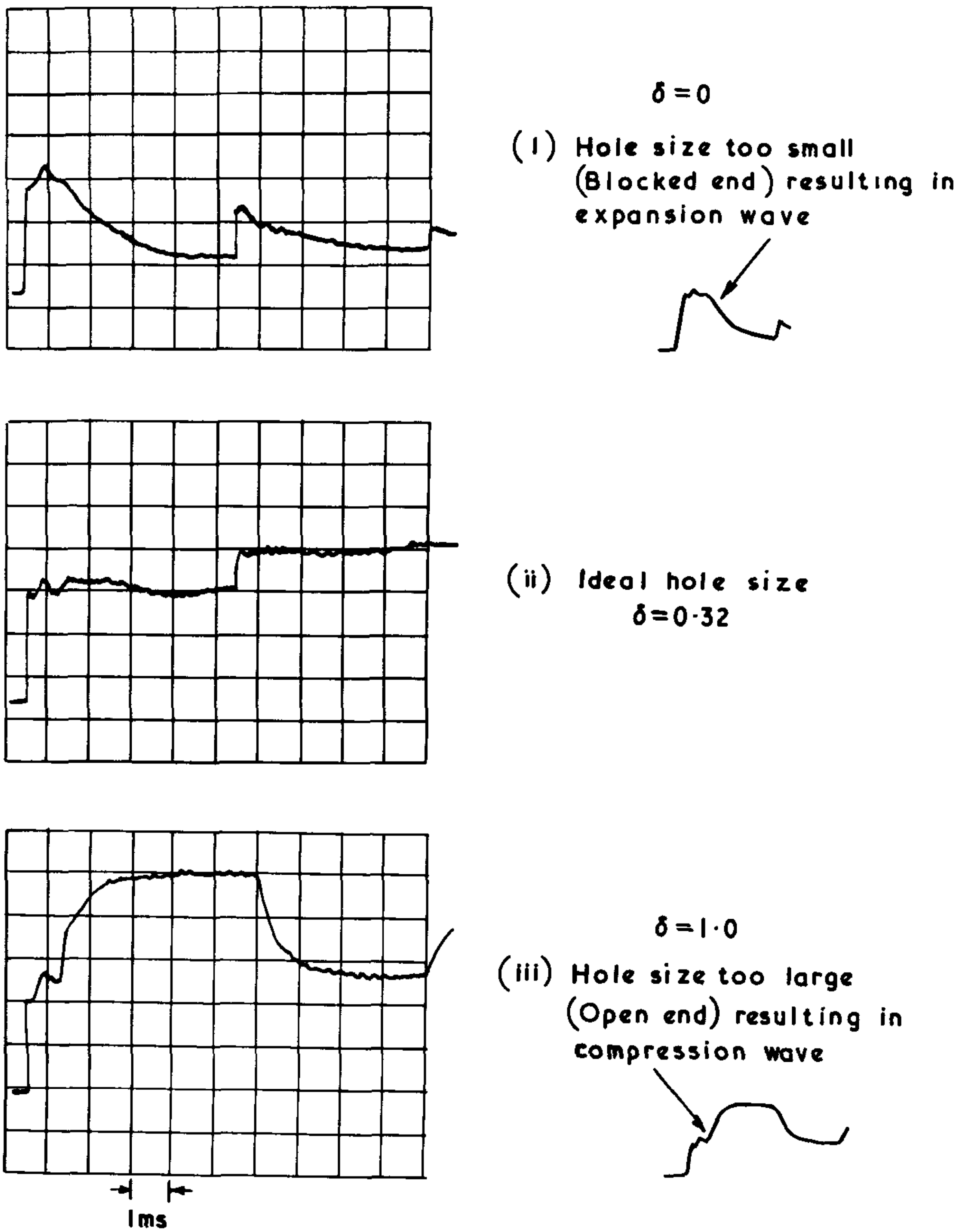

Determination of δ for Helium driver gas

FIG. 6

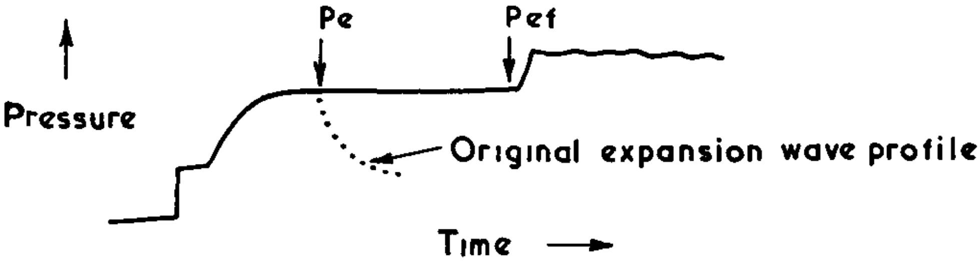

(i) Identification of pressure levels

In all cases
$M_s = 2,\ p_4 =$ atm pressure
Time base 5 m secs / air
Air as driver gas
Reservoir No. 1
$\frac{A_r}{A_t} = 10{\cdot}541$

Reservoir No. 2
$\frac{A_r}{A_t} = 47{\cdot}56$

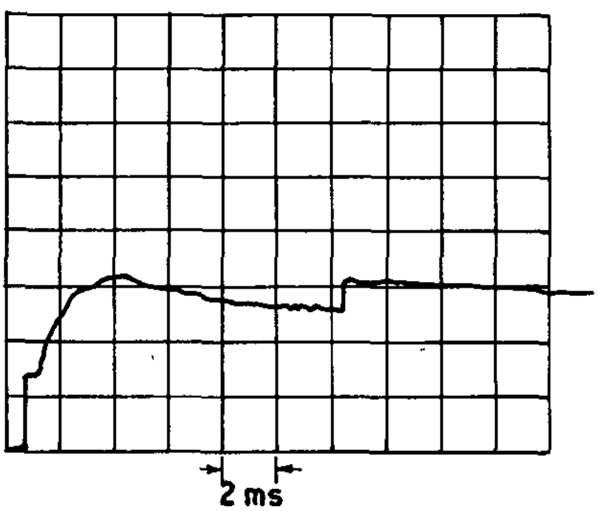

Determination of optimum reservoir cross-sectional area

FIG. 6 (cont.)

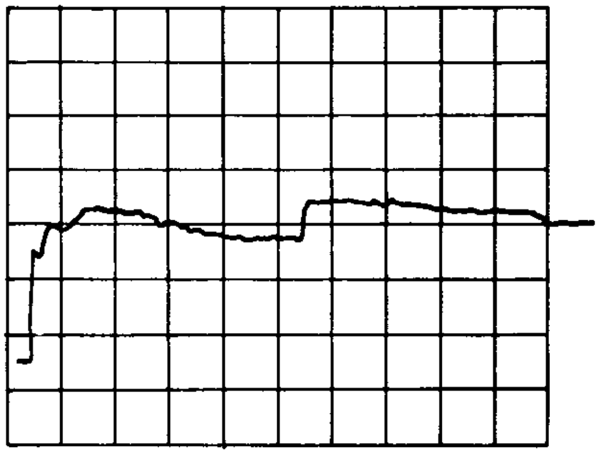

Reservoir No. 2

$\frac{A_r}{A_t} = 50$

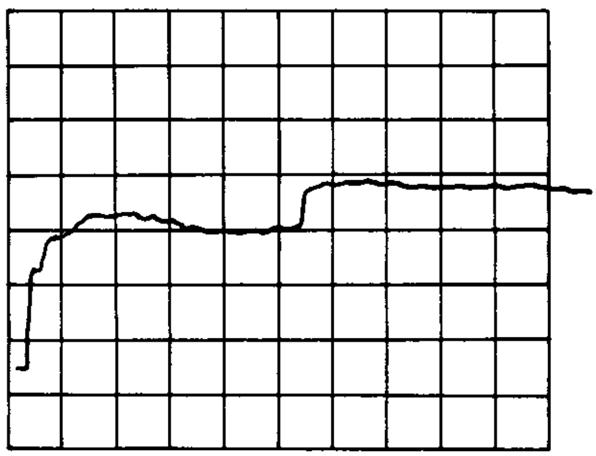

Reservoir No. 3

$\frac{A_r}{A_t} = 107$

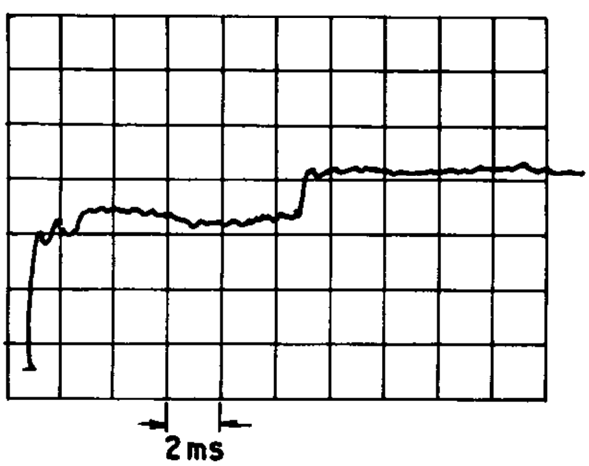

Reservoir No. 6

$\frac{A_r}{A_t} = 250$ (About the ideal value)

Minimum area ratio

Determination of optimum A_r/A_t for helium driver gas

FIG 6 (cont.)

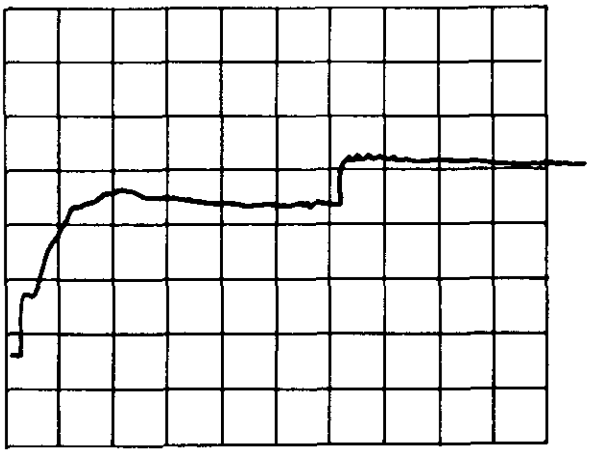

Reservoir No.3

$\frac{A_r}{A_t}$ = 107·02 (i.e about the ideal value)

Minimum area ratio for

$P_e \approx P_{ef}$

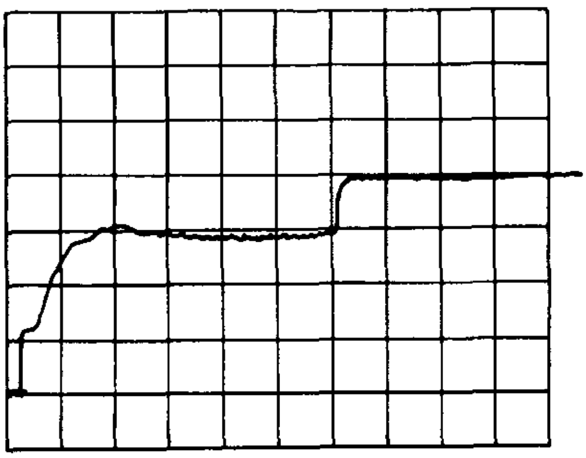

Reservoir No. 6

$\frac{A_r}{A_t}$ = 247·3

No significant improvement over reservoir No. 3

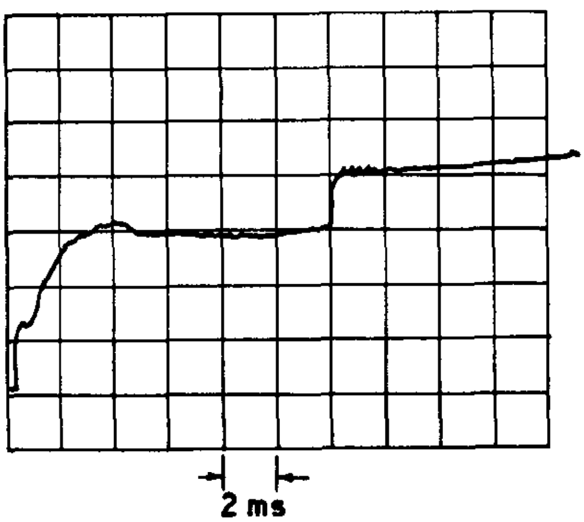

Infinite case

$\frac{A_r}{A_t} = \infty$

No significant improvement over reservoir No.3

Air as driver gas

FIG. 7

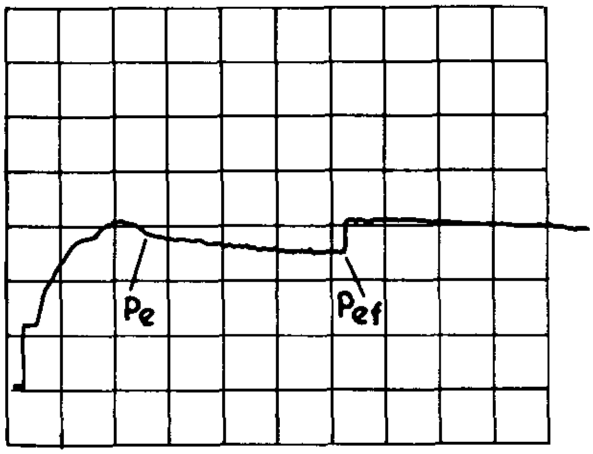

Length = 6 in., Reservoir No 3 (a) shows fall in pressure $p_e - p_{ef}$ due to drop in reservoir pressure

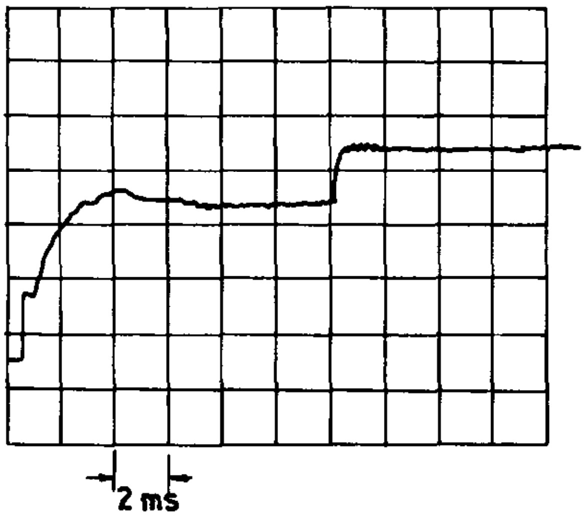

Length = 24 in., Reservoir No. 3 (b) no significant improvement over reservoir No. 3 (see Fig. 6) where length = 12 in.

Effects of reservoir length. $M_s = 2\cdot 0$ p_4 = atm pressure. (Air) $\frac{A_r}{A_t} = 107$

FIG. 8 (a)

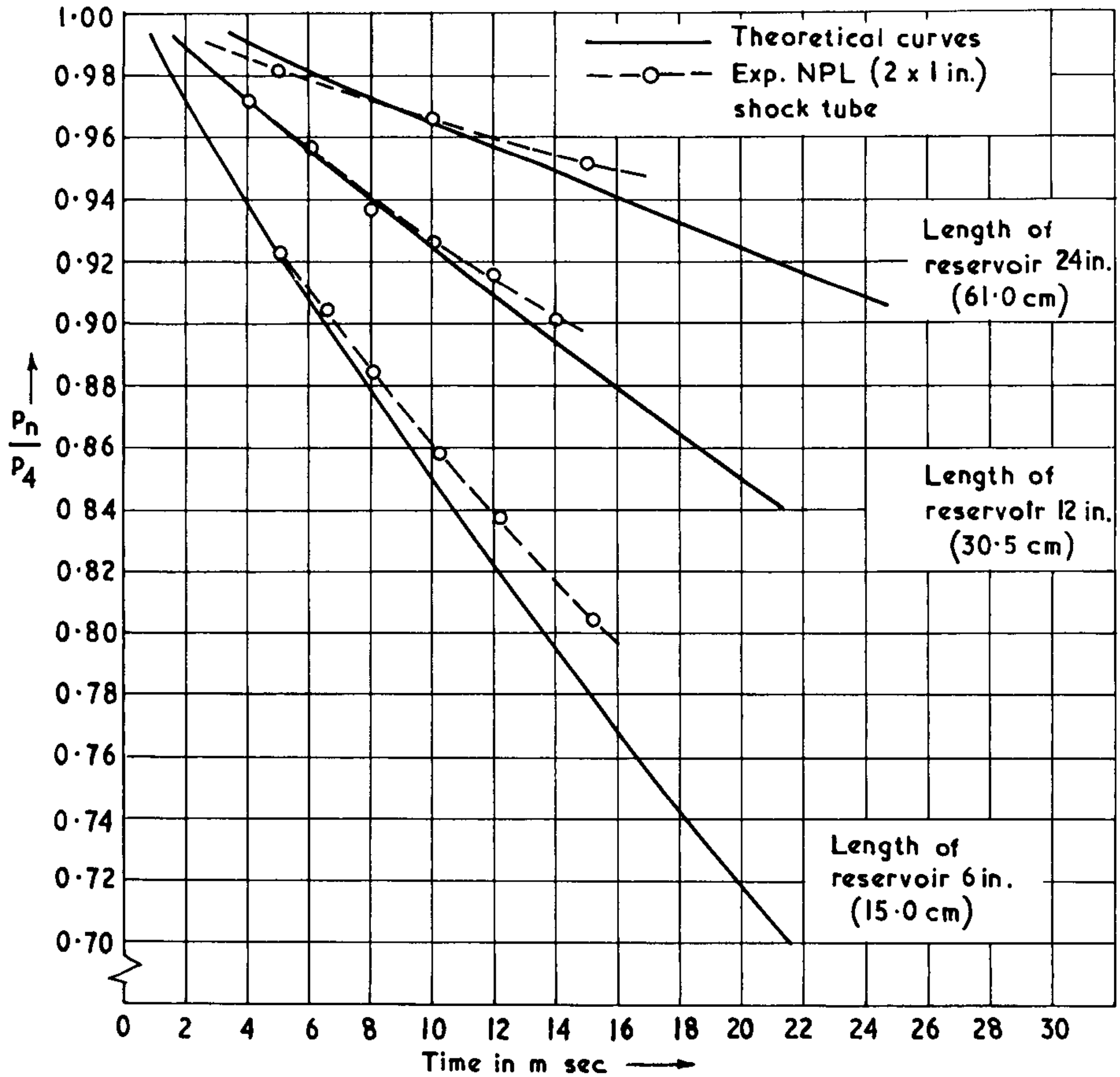

Comparison between experimental and theoretical values of p_n/p_4 vs time for reservoirs 3, 3a and 3b $A_r/A_t = 107 \cdot 2$, $\gamma = 1 \cdot 4$ (Air)

FIG. 8 (b)

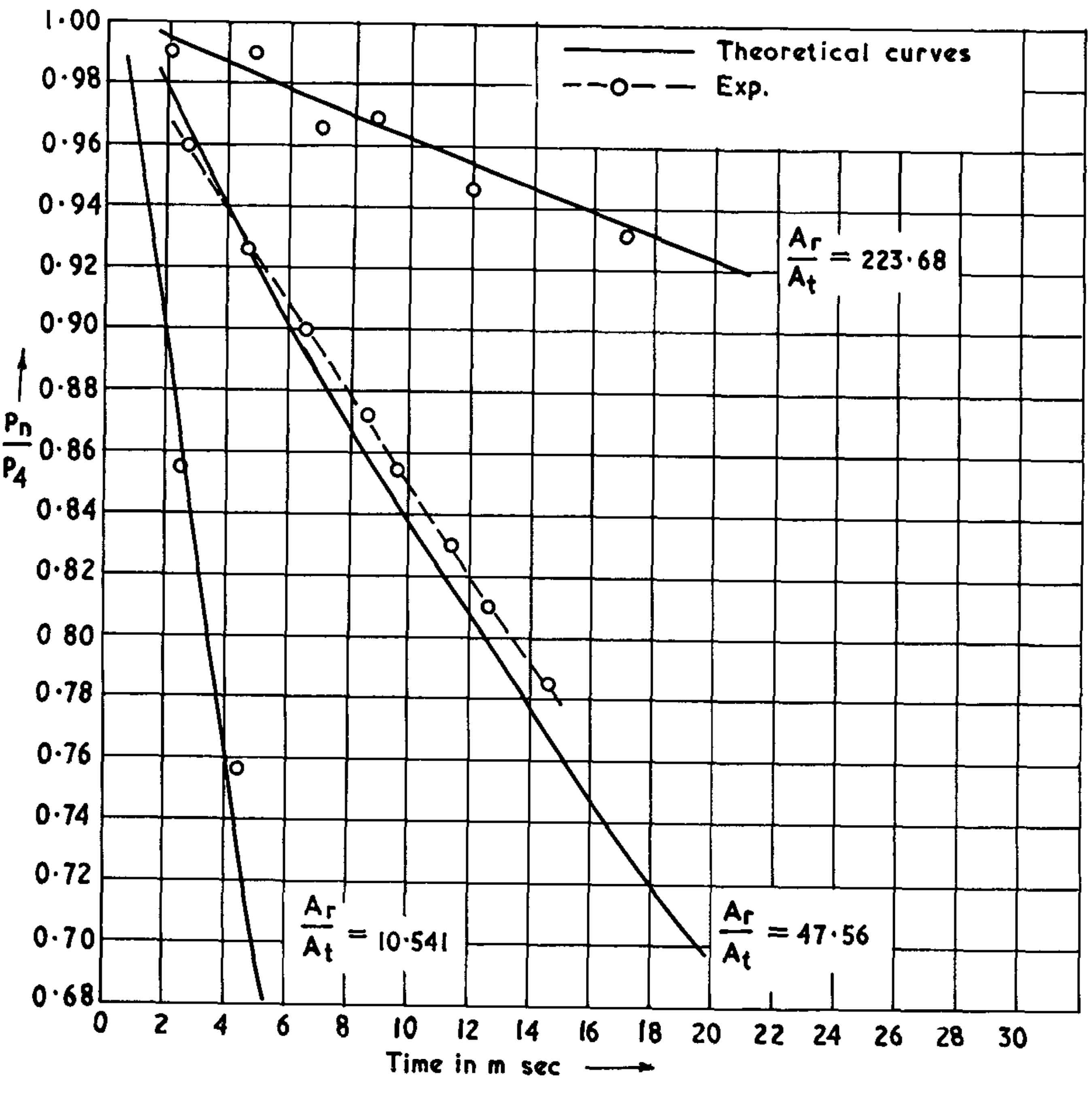

Comparison between experimental and theoretical values of p_4/p_1 vs time

$\gamma = 1{\cdot}4$ (Air)

FIG. 8(c)

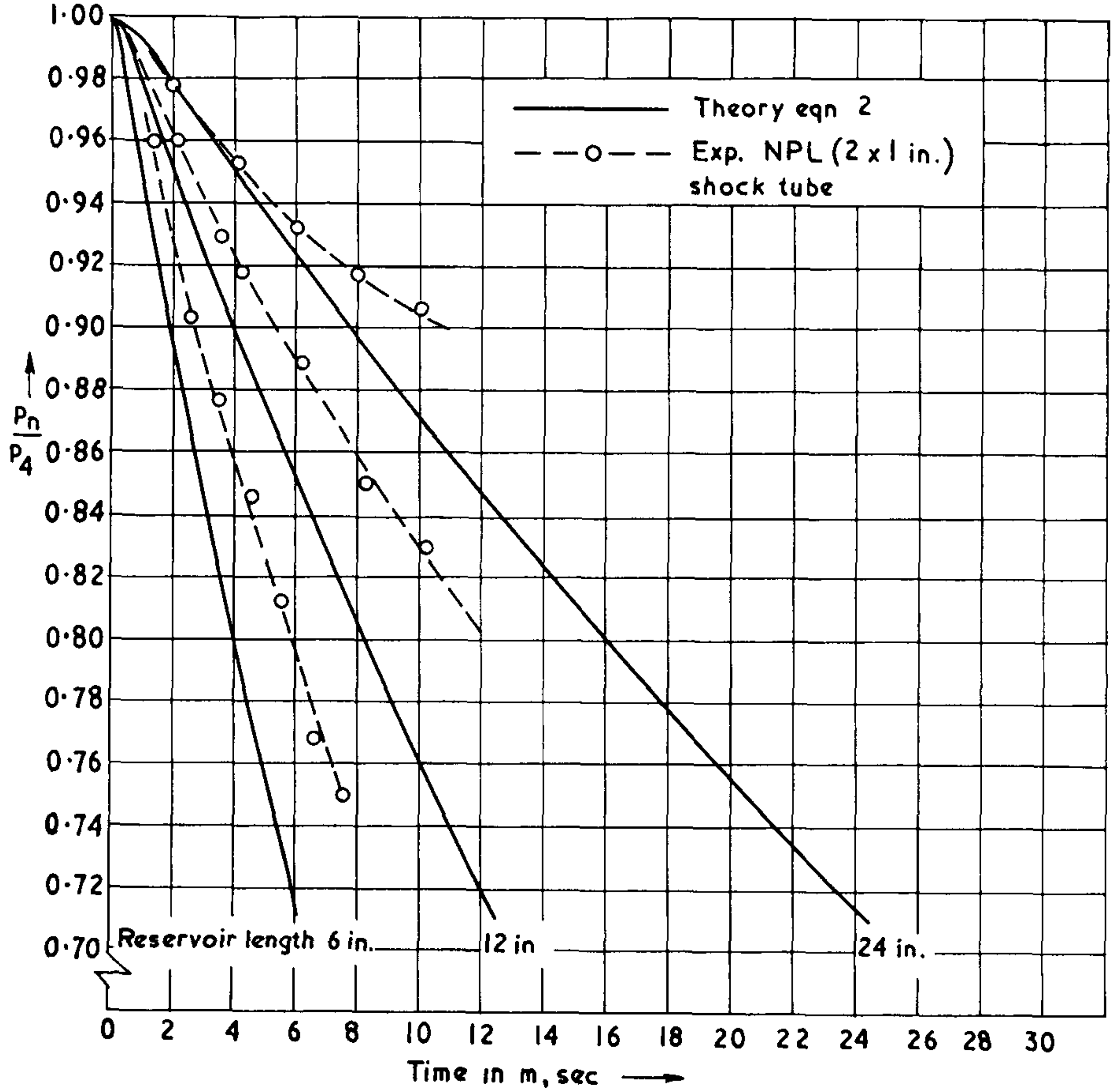

Comparison between experimental and theoretical values of p_n/p_4 vs time for reservoirs 3, 3a and 3b. $A_r/A_t = 100$, $\gamma = 1{\cdot}66$, He

FIG. 8 (d)

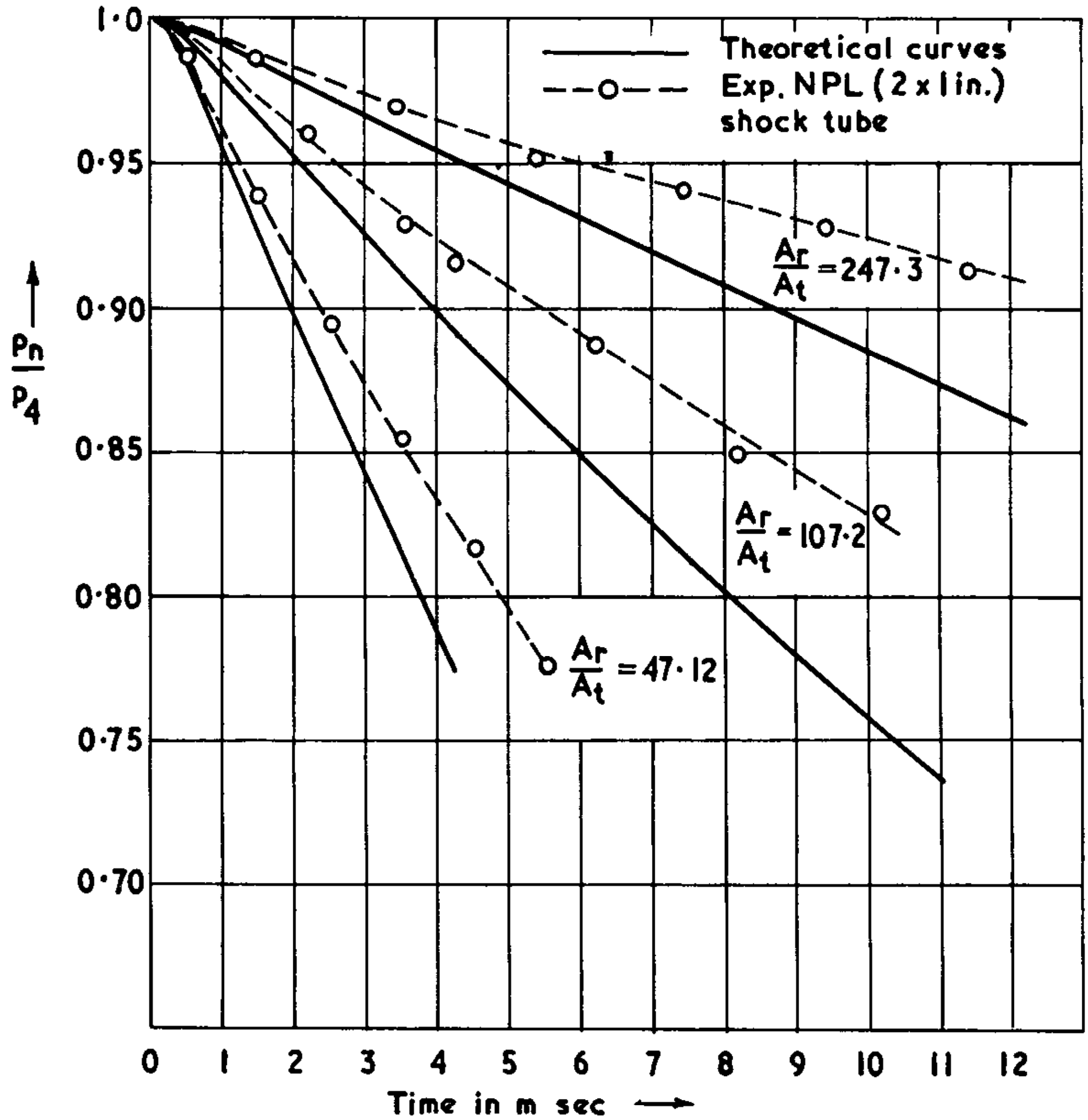

Comparison between experimental and theoretical values of p_n/p_4 vs time for reservoirs 2, 3 and 6 γ 1·667 (He)

D 106849/1/135645 K.3 9/68 P

A.R.C. C.P. No.1019
January 1968

Davies, L., Brown, D. R. and Hooper, G.

ON THE DRIVER-RESERVOIR TECHNIQUE
PART 1. APPLICATION TO SHOCK AND GUN TUNNELS
PART 2. DETERMINATION OF OPTIMUM RESERVOIR SIZE

The driver-reservoir technique is used when an increase in running time is required in shock or gun tunnels. The increase is achieved by effectively eliminating the reflected head of the expansion wave produced when the main diaphragm bursts. A theoretical and experimental appraisal is given of the application of the technique in situations of practical interest, and a method is described for the determination of optimum reservoir size to ensure efficient use of the technique.

A.R.C. C.P. No.1019
January 1968

Davies, L., Brown, D.R. and Hooper, G.

ON THE DRIVER-RESERVOIR TECHNIQUE
PART 1. APPLICATION TO SHOCK AND GUN TUNNELS
PART 2. DETERMINATION OF OPTIMUM RESERVOIR SIZE

The driver-reservoir technique is used when an increase in running time is required in shock or gun tunnels. The increase is achieved by effectively eliminating the reflected head of the expansion wave produced when the main diaphragm bursts. A theoretical and experimental appraisal is given of the application of the technique in situations of practical interest, and a method is described for the determination of optimum reservoir size to ensure efficient use of the technique.

A.R.C. C.P. No.1019
January 1968

Davies, L., Brown, D. R. and Hooper, G.

ON THE DRIVER-RESERVOIR TECHNIQUE
PART 1. APPLICATION TO SHOCK AND GUN TUNNELS
PART 2. DETERMINATION OF OPTIMUM RESERVOIR SIZE

The driver-reservoir technique is used when an increase in running time is required in shock or gun tunnels. The increase is achieved by effectively eliminating the reflected head of the expansion wave produced when the main diaphragm bursts. A theoretical and experimental appraisal is given of the application of the technique in situations of practical interest, and a method is described for the determination of optimum reservoir size to ensure efficient use of the technique.

DETACHABLE ABSTRACT CARDS

C.P. No. 1019

Printed and published by
HER MAJESTY'S STATIONERY OFFICE

To be purchased from
49 High Holborn, London W C 1
13A Castle Street, Edinburgh 2
109 St Mary Street, Cardiff CF1 1JW
Brazennose Street, Manchester 2
50 Fairfax Street, Bristol BS1 3DE
258 Broad Street, Birmingham 1
7 Linenhall Street, Belfast BT2 8AY
or through any bookseller

Printed in England

C.P. No. 1019

S O Code No 23-9018-19